

Noise-Induced Barren Plateaus in Variational Quantum Algorithms

Samson Wang,^{1,2} Enrico Fontana,^{1,3,4} M. Cerezo,^{1,5} Kunal Sharma,^{1,6}
Akira Sone,^{1,5} Lukasz Cincio,¹ and Patrick J. Coles¹

¹ *Theoretical Division, Los Alamos National Laboratory, Los Alamos, NM 87545, USA*

² *Imperial College London, London, UK*

³ *University of Strathclyde, Glasgow, UK*

⁴ *National Physical Laboratory, Teddington, UK*

⁵ *Center for Nonlinear Studies, Los Alamos National Laboratory, Los Alamos, NM, USA*

⁶ *Hearne Institute for Theoretical Physics and Department of Physics and Astronomy,
Louisiana State University, Baton Rouge, LA USA*

Variational Quantum Algorithms (VQAs) may be a path to quantum advantage on Noisy Intermediate-Scale Quantum (NISQ) computers. A natural question is whether the noise on NISQ devices places any fundamental limitations on the performance of VQAs. In this work, we rigorously prove a serious limitation for noisy VQAs, in that the noise causes the training landscape to have a barren plateau (i.e., vanishing gradient). Specifically, for the local Pauli noise considered, we prove that the gradient vanishes exponentially in the number of layers L . This implies exponential decay in the number of qubits n when L scales as $\text{poly}(n)$, for sufficiently large coefficients in the polynomial. These noise-induced barren plateaus (NIBPs) are conceptually different from noise-free barren plateaus, which are linked to random parameter initialization. Our result is formulated for an abstract ansatz that includes as special cases the Quantum Alternating Operator Ansatz (QAOA) and the Unitary Coupled Cluster Ansatz, among others. In the case of the QAOA, we implement numerical heuristics that confirm the NIBP phenomenon for a realistic hardware noise model.

I. Introduction

One of the great unanswered technological questions is whether Noisy Intermediate Scale Quantum (NISQ) computers will yield a quantum advantage for tasks of practical interest [1]. At the heart of this discussion are Variational Quantum Algorithms (VQAs), which are believed to be the best hope for near-term quantum advantage [2]. Such algorithms leverage classical optimizers to train the parameters in a quantum circuit, while employing a quantum device to efficiently estimate an application-specific cost function or its gradient. By keeping the quantum circuit depth relatively short, VQAs mitigate hardware noise and may enable near-term applications including electronic structure [3–5], dynamics [6–9], optimization [10–13], linear systems [14, 15], metrology [16], factoring [17], compiling [18–20], and others [21–25].

The main open question for VQAs is their scalability to large problem sizes. While performing numerical heuristics for small or intermediate problem sizes is the norm for VQAs, deriving analytical scaling results is rare for this field. Noteworthy exceptions are some recent studies of the scaling of the gradient in VQAs with the number of qubits n [26–29]. Namely, it was proven of that the gradient vanishes exponentially in n for randomly initialized, deep Hardware Efficient ansatzes [26] and dissipative quantum neural networks [27], and also for shallow depth with global cost functions [28]. This vanishing gradient phenomenon is now referred to as barren plateaus in the training landscape. Fortunately, investigations into barren plateaus have spawned several promising strategies to avoid them, including local cost functions [28], parameter correlation [29], pre-training [30], and layer-by-layer training [31, 32]. Such strategies give hope that

perhaps VQAs may avoid the exponential scaling that otherwise would result from the exponential precision requirements of navigating through a barren plateau.

However, these works do not consider quantum hardware noise, and very little is known about the scalability of VQAs in the presence of noise. One of the main selling points of VQAs is noise mitigation, and indeed VQAs have shown evidence of noise resilience in the sense that the global minimum of the landscape may be unaffected by noise [2, 19]. While some analysis has been done [33–35], an important open question, which has not yet been addressed, is how noise affects the asymptotic scaling of VQAs. More specifically, one can ask how noise affects the training process. Intuitively, incoherent noise is expected to reduce the magnitude of the gradient and hence hinder trainability, and preliminary numerical evidence of this has been seen [36, 37], although the scaling of this effect has not been studied.

In this work, we analytically study the scaling of gradient for VQAs as a function of n , the circuit depth L , and a noise parameter q . We consider a general class of local noise models that includes depolarizing noise and certain kinds of Pauli noise. Furthermore, we investigate a general, abstract ansatz that allows us to encompass many of the important ansatzes in the literature, hence allowing us to make a general statement about VQAs. This includes the Quantum Alternating Operator Ansatz (QAOA) which is used for solving combinatorial optimization problems [10–13], the Unitary Coupled Cluster (UCC) Ansatz which is used in the Variational Quantum Eigensolver (VQE) for chemistry [38–40], and the Hardware Efficient Ansatz which is employed for various applications [41–43].

Our main result (Theorem 1) is an upper bound on the

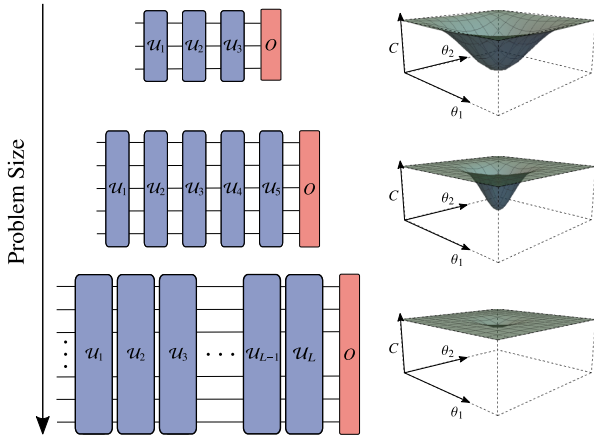


FIG. 1. **Schematic diagram of the Noise-Induced Barren Plateau (NIBP) phenomenon.** For various applications such as chemistry and optimization, increasing the problem size often requires one to increase the depth L of the variational ansatz. We show that, in the presence of local noise, the gradient vanishes exponentially in L and hence exponentially in the number of qubits n when L scales as a sufficiently large polynomial in n . This can be seen in the plots on the right, which show the cost function landscapes for a simple variational problem with local noise.

magnitude of the gradient that decays exponentially with L , namely as $2^{-\kappa}$ with $\kappa = L \log_2(q) - n/2$. Hence we find that the gradient vanishes exponentially in the circuit depth. Moreover, it is typical to consider L scaling as $\text{poly}(n)$ (e.g., in the UCC Ansatz [40]), and for sufficiently large coefficients in this polynomial, our main result implies a barren plateau (exponential decay in n). We refer to this as a Noise-Induced Barren Plateau (NIBP). We remark that NIBPs can be viewed as a consequence of the cost landscape concentrating around the value of the cost for the maximally mixed state, and we make this precise in Lemma 1. See Fig. 1 for a schematic diagram of the NIBP phenomenon.

To be clear, any variational algorithm with a NIBP will have exponential scaling. In this sense, NIBPs destroy quantum speedup, as the standard goal of quantum algorithms is to avoid the typical exponential scaling of classical algorithms. NIBPs are conceptually distinct from the noise-free barren plateaus of Refs. [26–28]. Indeed, strategies to avoid noise-free barren plateaus [28–32] do not appear to solve the NIBPs issue. The obvious strategy to address NIBPs is error reduction, i.e., to increase the noise parameter q (decrease the noise strength). Hence, our work provides quantitative guidance for how large q needs to be to potentially avoid NIBPs.

In what follows, we present our general framework followed by our main result. We also present two extensions of our main result, one involving correlated ansatz parameters and one allowing for measurement noise. The latter indicates that global cost functions exacerbate the NIBP issue. In addition, we provide numerical heuristics

that illustrate our main result for MaxCut optimization with the QAOA, showing that NIBPs significantly impact this application.

II. Results

A. General Framework

In this work we analyze a general class of parameterized ansatzes $U(\boldsymbol{\theta})$ that can be expressed as a product of L unitaries sequentially applied by layers

$$U(\boldsymbol{\theta}) = U_L(\boldsymbol{\theta}_L) \cdots U_2(\boldsymbol{\theta}_2) \cdot U_1(\boldsymbol{\theta}_1). \quad (1)$$

Here $\boldsymbol{\theta} = \{\boldsymbol{\theta}_l\}_{l=1}^L$ is a set of vectors of continuous parameters that are optimized to minimize a cost function C that can be expressed as the expectation value of an operator O :

$$C = \text{Tr}[OU(\boldsymbol{\theta})\rho U^\dagger(\boldsymbol{\theta})]. \quad (2)$$

As shown in Fig. 2, ρ is an n -qubit input state. Without loss of generality we assume that each $U_l(\boldsymbol{\theta}_l)$ is given by

$$U_l(\boldsymbol{\theta}_l) = \prod_m e^{-i\theta_{lm} H_{lm}} W_{lm}, \quad (3)$$

where H_{lm} are Hermitian operators, $\boldsymbol{\theta}_l = \{\theta_{lm}\}$ are continuous parameters, and W_{lm} denote unparametrized gates. We expand H_{lm} and O in the Pauli basis as

$$H_{lm} = \boldsymbol{\eta}_{lm} \cdot \boldsymbol{\sigma}_n = \sum_i \eta_{lm}^i \sigma_n^i, \quad O = \boldsymbol{\omega} \cdot \boldsymbol{\sigma}_n = \sum_i \omega^i \sigma_n^i, \quad (4)$$

where $\sigma_n^i \in \{\mathbb{1}, X, Y, Z\}^{\otimes n}$ are Pauli strings, and $\boldsymbol{\eta}_{lm}$ and $\boldsymbol{\omega}$ are real-valued vectors that specify the terms present in the expansion. Defining $N_{lm} = |\boldsymbol{\eta}_{lm}|$ and $N_O = |\boldsymbol{\omega}|$ as the number of non-zero elements, i.e., the number of terms in the summations in Eq. (4), we say that H_{lm} and O admit an efficient decomposition if $N_{lm}, N_O \in \mathcal{O}(\text{poly}(n))$, respectively.

We now briefly discuss how the QAOA, UCC, and Hardware Efficient ansatzes fit into this general framework. We refer the reader to the Methods section for additional details. In QAOA one sequentially alternates the action of two unitaries as

$$U(\boldsymbol{\gamma}, \boldsymbol{\beta}) = e^{-i\beta_p H_M} e^{-i\gamma_p H_P} \cdots e^{-i\beta_1 H_M} e^{-i\gamma_1 H_P}, \quad (5)$$

where H_P and H_M are the so-called problem and mixer Hamiltonian, respectively. We define N_P (N_M) as the number of terms in the Pauli decomposition of H_P (H_M). On the other hand, Hardware Efficient ansatzes naturally fit into Eqs. (1)–(3) as they are usually composed of fixed gates (e.g, controlled NOTs), and parametrized gates (e.g., single qubit rotations). Finally, as detailed in the Methods, the UCC ansatz can be expressed as

$$U(\boldsymbol{\theta}) = \prod_{lm} U_{lm}(\theta_{lm}) = \prod_{lm} e^{i\theta_{lm} \sum_i \mu_{lm}^i \sigma_n^i}, \quad (6)$$

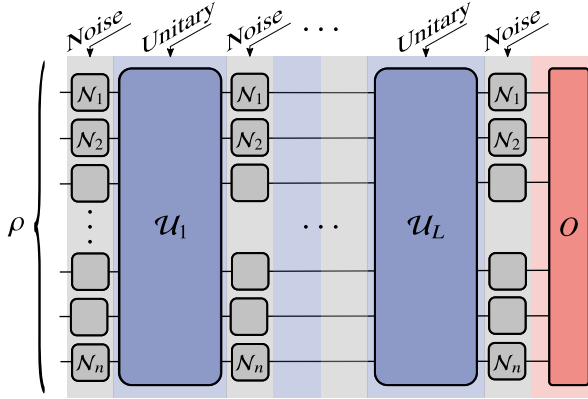


FIG. 2. **Setting for our analysis.** An n -qubit input state ρ is sent through a variational ansatz $U(\theta)$ composed of L unitary layers $U_l(\theta_l)$ sequentially acting according to Eq. (1). Here, \mathcal{U}_l denotes the quantum channel that implements the unitary $U_l(\theta_l)$. The parameters in the ansatz $\theta = \{\theta_l\}_{l=1}^L$ are trained to minimize a cost function that is expressed as the expectation value of an operator O as in Eq. (2). We consider a noise model where local Pauli noise channels \mathcal{N}_j act on each qubit j before and after each unitary.

where $\mu_{lm}^i \in \{0, \pm 1\}$, and where θ_{lm} are the coupled cluster amplitudes. Moreover, we denote $\hat{N}_{lm} = |\mu_{lm}|$ as the number of non-zero elements in $\sum_i \mu_{lm}^i \sigma_n^i$.

As shown in Fig. 2, we consider a noise model where local Pauli noise channels \mathcal{N}_j act on each qubit j before and after each unitary $U_l(\theta_l)$. The action of \mathcal{N}_j on a local Pauli operator $\sigma \in \{X, Y, Z\}$ can be expressed as

$$\mathcal{N}_j(\sigma) = q_\sigma \sigma, \quad (7)$$

where $-1 < q_X, q_Y, q_Z < 1$. Here, we characterize the noise strength with a single parameter $q = \max\{|q_X|, |q_Y|, |q_Z|\}$. Let \mathcal{U}_l denote the channel that implements the unitary $U_l(\theta_l)$ and let $\mathcal{N} = \mathcal{N}_1 \otimes \dots \otimes \mathcal{N}_n$ denote the n -qubit noise channel. Then, the noisy cost function is given by

$$\tilde{C} = \text{Tr} [O (\mathcal{N} \circ \mathcal{U}_L \circ \dots \circ \mathcal{N} \circ \mathcal{U}_1 \circ \mathcal{N})(\rho)]. \quad (8)$$

B. General Analytical Results

There are some VQAs, such as the VQE [3] for chemistry and other physical systems, where it is important to accurately characterize the value of the cost function itself. We provide an important result below in Lemma 1 that quantitatively bounds the cost function itself, and we envision that this bound will be especially useful in the context of VQE. On the other hand, there are other VQAs, such as those for optimization [10–13], compiling [18–20], and linear systems [14, 15], where the key goal is to learn the optimal parameters and the precise value of the cost function is either not important or can be computed classically after learning the parameters.

In this case, one is primarily concerned with trainability, and hence the gradient is a key quantity of interest. These applications motivate our main result in Theorem 1, which bounds the magnitude of the gradient. We remark that trainability is of course also important for VQE, and hence Theorem 1 is also of interest for this application.

With this motivation in mind, we now present our main results. We first present our bound on the cost function, since one can view this as a lemma that provides an explanation for the origin of our main theorem. Namely, in the following lemma, we show that the cost function concentrates around the corresponding value for the maximally mixed state.

Lemma 1 (Concentration of the cost function). *Consider an L -layered ansatz of the form in Eq. (1). Suppose that local Pauli noise of the form of Eq. (7) with noise strength q acts before and after each layer as in Fig. 2. Then, for a cost function \tilde{C} of the form in Eq. (8), the following bound holds*

$$\left| \tilde{C} - \frac{1}{2^n} \text{Tr}[O] \right| \leq G(n) \quad (9)$$

where

$$G(n) = N_O \|\omega\|_\infty 2^{n/2} q^{L+1}. \quad (10)$$

Here $\|\cdot\|_\infty$ is the infinity norm, ω is defined in Eq. (4) and $N_O = |\omega|$ is the number of non-zero elements in the Pauli decomposition of O .

This lemma implies the cost landscape exponentially concentrates on the value $\text{Tr}[O]/2^n$ for large n , whenever L scales as a sufficiently large polynomial in n . For example, if L scales linearly with n , i.e. $\exists t > 0$, such that $L = tn$, then our bound implies that this effect will occur if the noise exceeds a threshold: $q \leq 2^{-(c+1/2t)}$, where $c > 0$. If the depth is superlinear in n , then the exponential concentration of the cost is guaranteed for any value of the noise strength. While this lemma has important applications on its own, particularly for VQE, it also provides intuition for the origin of the NIBP phenomenon, which we now state.

Let $\partial_{lm} \tilde{C} = \partial \tilde{C} / \partial \theta_{lm}$ denote the partial derivative of the noisy cost function with respect to the m -th parameter that appears in the l -th layer of the ansatz, as in Eq. (3). For our main technical result, we upper bound $|\partial_{lm} \tilde{C}|$ as a function of L and n .

Theorem 1 (Upper bound on the partial derivative). *Consider an L -layered ansatz as defined in Eq. (1). Let θ_{lm} denote the trainable parameter corresponding to the Hamiltonian H_{lm} in the unitary $U_l(\theta_l)$ appearing in the ansatz. Suppose that local Pauli noise of the form in Eq. (7) with noise parameter q acts before and after each layer as in Fig. 2. Then the following bound holds for the partial derivative of the noisy cost function*

$$|\partial_{lm} \tilde{C}| \leq F(n), \quad (11)$$

where

$$F(n) = \sqrt{2} N_{lm} N_O \|\boldsymbol{\eta}_{lm}\|_\infty \|\boldsymbol{\omega}\|_\infty 2^{n/2} q^{L+1}, \quad (12)$$

and $\boldsymbol{\eta}_{lm}$ and $\boldsymbol{\omega}$ are defined in Eq. (4), with respective number of non-zero elements N_{lm} and N_O .

Let us now consider the asymptotic scaling of the function $F(n)$ in Eq. (12). Under standard assumptions such as that H_{lm} and O in Eq. (4) admit efficient Pauli decompositions, we now state that $F(n)$ decays exponentially in n , if L grows sufficiently quickly with n .

Corollary 1 (Noise-induced barren plateaus). *Let $N_{lm}, N_O \in \mathcal{O}(\text{poly}(n))$ and let $\boldsymbol{\eta}_{lm}^i, \boldsymbol{\omega}^j \in \mathcal{O}(\text{poly}(n))$ for all i, j . Then the upper bound $F(n)$ in Eq. (12) vanishes exponentially in n as*

$$F(n) \in \mathcal{O}(2^{-\alpha n}), \quad (13)$$

if $\exists c \in \mathbb{R}$ and $\exists n_0$ such that $\forall n \geq n_0$,

$$L \geq \frac{1}{\log_2(q)} \left(\alpha + \frac{1}{2} \right) n - c. \quad (14)$$

Note that the asymptotic scaling in Eq. (13) is independent of l and m , i.e., the scaling is blind to the layer, or the parameter within the layer, for which the derivative is taken. Hence, this corollary implies that, when Eq. (14) holds, the partial derivative $|\partial_{lm} \tilde{C}|$ exponentially vanishes in n across the entire cost landscape. In other words, one observes a Noise-Induced Barren Plateau (NIBP) for all points on the landscape. Furthermore, note that if L is superlinear in n , then Eq. (14) is satisfied for all $q < 1$. Hence, in this case, NIBPs occur regardless of the noise strength.

In addition, Corollary 1 implies that NIBPs are conceptually different from noise-free barren plateaus. First, NIBPs are independent of the parameter initialization strategy or the locality of the cost function. Second, NIBPs exhibit exponential decay of the gradient itself; not just of the variance of the gradient, which is the hallmark of noise-free barren plateaus. Noise-free barren plateaus allow the global minimum to sit inside deep, narrow valley in the landscape [28], whereas NIBPs flatten the entire landscape.

One of the strategies to avoid the noise-free barren plateaus is to correlate parameters, i.e., to make a subset of the parameters equal to each other [29]. We generalize Theorem 1 in the following remark to accommodate such a setting, consequently showing that such correlated or degenerate parameters do not help in avoiding NIBPs. In this setting, the result we obtain in Eq. (16) below is essentially identical to that in Eq. (12) except with an additional factor quantifying the amount of degeneracy.

Remark 1 (Degenerate parameters). *Consider the ansatz defined in Eqs. (1) and (3). Suppose there is a subset G_{st} of the set $\{\theta_{lm}\}$ in this ansatz such that G_{st} consists of b parameters that are degenerate:*

$$G_{st} = \{\theta_{lm} \mid \theta_{lm} = \theta_{st}\}. \quad (15)$$

Here, θ_{st} denotes the parameter in G_{st} for which $N_{lm} \|\boldsymbol{\eta}_{lm}\|_\infty$ takes the largest value in the set. (θ_{st} can also be thought of as a reference parameter to which all other parameters are set equal in value.) Then the partial derivative of the noisy cost with respect to θ_{st} is bounded as

$$|\partial_{st} \tilde{C}| \leq \sqrt{2} b N_{st} N_O \|\boldsymbol{\eta}_{st}\|_\infty \|\boldsymbol{\omega}\|_\infty 2^{n/2} q^{L+1} \quad (16)$$

at all points in the cost landscape.

Remark 1 is especially important in the context of the QAOA and the UCC ansatz, as discussed below. More generally, we note that a unitary of the form of Eq. (3) cannot generically be implemented as a single gate on a physical device. In practice one needs to compile the unitary into a sequence of native gates. Moreover, Hamiltonians with non-commuting terms are usually approximated with techniques such as Trotterization. This compilation overhead potentially leads to a sequence of gates that grows with n . Remark 1 enables us to account for such scenarios, and we elaborate on its relevance to specific applications in the next subsection.

Finally, we present an extension of our main result to the case of measurement noise. Consider a model of measurement noise where each local measurement independently has some bit-flip probability given by $(1 - q_M)/2$, which we assume to be symmetric with respect to the 0 and 1 outcomes. This leads to an additional reduction of our bounds on the cost function and its gradient that depends on the locality of the observable O .

Proposition 1 (Measurement noise). *Consider expanding the observable O as a sum of Pauli strings, as in Eq. (4). Let w denote the minimum weight of these strings, where the weight is defined as the number of non-identity elements for a given string. In addition to the noise process considered in Fig. 2, suppose there is also measurement noise consisting of a tensor product of local bit-flip channels with $(1 - q_M)/2$ being the bit-flip probability. Then we have*

$$\left| \tilde{C} - \frac{1}{2^n} \text{Tr}[O] \right| \leq q_M^w G(n) \quad (17)$$

and

$$|\partial_{lm} \tilde{C}| \leq q_M^w F(n) \quad (18)$$

where $G(n)$ and $F(n)$ are defined in Lemma 1 and Theorem 1, respectively.

Proposition 1 goes beyond the noise model considered in Theorem 1. It shows that in the presence of measurement noise there is an additional contribution from the locality of the measurement operator. It is interesting to draw a parallel between Proposition 1 and noise-free barren plateaus, which have been shown to be cost-function dependent and in particular depend on the locality of the observable O [28]. Similarly, the bounds in Proposition 1

depend on the locality of O . For example, when $w = n$, i.e., global observables, the factor q_M^w will hasten the exponential decay. On the other hand, when $w = 1$, i.e., local observables, the scaling is unaltered by measurement noise. In this sense, a global observable exacerbates the NIBP issue by making the decay more rapid with n .

C. Application-Specific Analytical Results

Here we investigate the implications of our results from Section II B for two applications: optimization and chemistry. In particular, we derive conditions for NIBPs for these applications. These conditions are derived in the setting where Trotterization is used, but other compilation strategies incur similar asymptotic behavior. We begin with the QAOA for optimization and then discuss the UCC ansatz for chemistry.

Corollary 2 (Example: QAOA). *Consider the QAOA with $2p$ trainable parameters, as defined in Eq. (5). Suppose that the implementation of unitaries corresponding to the problem Hamiltonian H_P and the mixer Hamiltonian H_M require k_P - and k_M -depth circuits, respectively. If local Pauli noise of the form in Eq. (7) with noise parameter q acts before and after each layer of native gates, then we have*

$$|\partial_{\beta_l} \tilde{C}| \leq \sqrt{2} b_{l,P} N_P \|\boldsymbol{\eta}_P\|_\infty \|\boldsymbol{\omega}\|_\infty 2^{n/2} q^{(k_P+k_M)p+1}, \quad (19)$$

$$|\partial_{\gamma_l} \tilde{C}| \leq \sqrt{2} b_{l,M} N_P \|\boldsymbol{\eta}_M\|_\infty \|\boldsymbol{\omega}\|_\infty 2^{n/2} q^{(k_P+k_M)p+1} \quad (20)$$

for any choice of parameters β_l, γ_l , and where $O = H_P$ in Eq. (2). Here $b_{l,P}$ and $b_{l,M}$ are the respective number of native gates parameterized by β_l and γ_l according to the compilation.

Corollary 2 follows from Remark 1 and it has interesting implications for the trainability of the QAOA. From Eqs. (19) and (20), NIBPs are guaranteed if $p k_P$ scales superlinearly in n , or if $p k_P$ scales linearly in n and the noise strength and number of rounds are above some threshold. This can manifest itself in a number of ways, which we explain below.

First, we look at the depth k_P required to implement one application of the problem unitary. Graph problems containing vertices of extensive degree such as the Sherrington-Kirkpatrick model inherently require $\Omega(n)$ depth to implement [43]. On the other hand, generic problems mapped to hardware topologies also have the potential to incur $\Omega(n)$ depth or greater in compilation cost. For instance, implementation of MaxCut and k -SAT using SWAP networks on circuits with 1-D connectivity requires depth $\Omega(n)$ and $\Omega(n^{k-1})$ respectively [12, 44]. Such mappings with the aforementioned compiling overhead could lead to NIBPs. For example, NIBPs are guaranteed for 3-SAT with any noise parameter q even for a fixed number of rounds p .

Second, it appears that p values that grow at least lightly with n may be needed for quantum advantage in certain optimization problems (for example, [45–47]). In

addition, there are problems employing the QAOA that explicitly require p scaling as $\text{poly}(n)$ [17, 48]. Thus, without even considering the compilation overhead for the problem unitary, these QAOA problems may run into NIBPs particularly when aiming for quantum advantage. Moreover, weak growth of p with n combined with compilation overhead could still result in an NIBP.

Finally, we note that above we have assumed the contribution of k_P dominates that of k_M . However, it is possible that for choice of more exotic mixers [13], k_M also needs to be carefully considered to avoid NIBPs.

Corollary 3 (Example: UCC). *Let H denote a molecular Hamiltonian of a system of M_e electrons. Consider the UCC ansatz as defined in Eq. (6). If local Pauli noise of the form in Eq. (7) with noise parameter q acts before and after every $U_{lm}(\theta_{lm})$ in Eq. (6), then we have*

$$|\partial_{\theta_{lm}} \tilde{C}| \leq \sqrt{2} \hat{N}_{lm} N_H \|\boldsymbol{\omega}\|_\infty 2^{n/2} q^{L+1}, \quad (21)$$

for any coupled cluster amplitude θ_{lm} , and where $O = H$ in Eq. (2).

Corollary 3 allows us to make general statements about the trainability of UCC ansatz. We present the details for the standard UCC ansatz with single and double excitations from occupied to virtual orbitals [38, 49] (see Methods for more details). Let M_o denote the total number of spin orbitals. Then at least $n = M_o$ qubits are required to simulate such a system and the number of variational parameters grows as $\Omega(n^2 M_e^2)$ [44, 50]. To implement the UCC ansatz on a quantum computer, the excitation operators are first mapped to Pauli operators using Jordan-Wigner or Bravyi-Kitaev mappings [51, 52]. Then, using first-order Trotterization and employing SWAP networks [44], the UCC ansatz can be implemented in $\Omega(n^2 M_e)$ depth, while assuming 1-D connectivity of qubits [44]. Hence for the UCC ansatz, approximated by single- and double-excitation operators, the upper bound in Eq. (21) (asymptotically) vanishes exponentially in n .

To target strongly correlated states for molecular Hamiltonians, one can employ a UCC ansatz that includes additional, generalized excitations [53, 54]. A $\Omega(n^3)$ depth circuit is required to implement the first-order Trotterized form of this ansatz [44]. Hence NIBPs become more prominent for generalized UCC ansatzes. Finally, we remark that a sparse version of the UCC ansatz can be implemented in $\Omega(n)$ depth [44]. NIBPs can occur for such ansatzes due to the requirement of higher-order Trotterization to obtain results within or close to chemical accuracy and for sufficiently high noise values.

D. QAOA Heuristics

To illustrate the NIBP phenomenon beyond the conditions assumed in our analytical results, we numerically implement the QAOA to solve MaxCut combinatorial optimization problems. We employ a realistic noise model

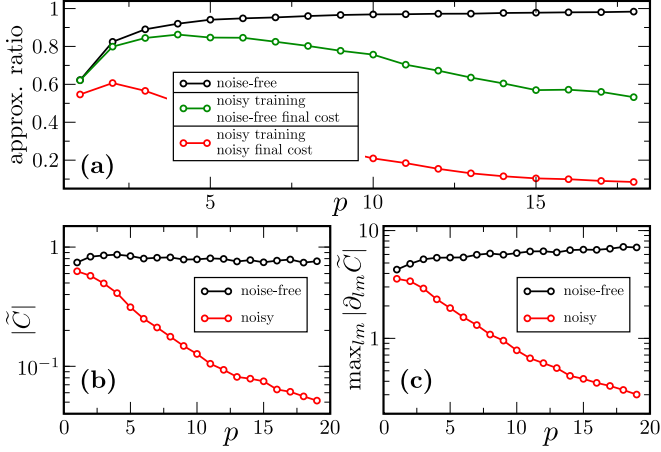


FIG. 3. **QAOA heuristics in the presence of realistic hardware noise.** The noise model used here was obtained from gate-set tomography of the IBM Ourense device. (a) The approximation ratio averaged over 100 random graphs of 5 nodes is plotted versus number of layers p . The black, green, and red curves respectively correspond to noise-free training, noisy training with noise-free final cost evaluation, and noisy training with noisy final cost evaluation. The performance of noise-free training increases with p . The green curve shows that the training process itself is hindered by noise, with the performance decreasing steadily with p for $p > 4$. (b) The absolute value of the cost function, averaged over graphs and parameter values, is plotted versus p . As p increases the cost decays approximately exponentially with p (linear on the log scale). (c) The absolute value of the largest partial derivative, averaged over graphs and parameter values, is plotted versus p . The partial derivatives decay approximately exponentially with p , showing evidence of Noise-Induced Barren Plateaus (NIBPs).

obtained from gate-set tomography on the IBM Ourense superconducting qubit device. In the Methods section we provide additional details on the noise model and the optimization method employed.

Let us first recall that a MaxCut problem is specified by a graph $G = (V, E)$ of nodes V and edges E . The goal is to partition the nodes of G into two sets which maximize the number of edges connecting nodes between sets. Here, the QAOA problem Hamiltonian is given by

$$H_P = \frac{1}{2} \sum_{ij} C_{ij} Z_i Z_j, \quad (22)$$

where Z_i are local Pauli operators on qubit (node) i , and where $C_{ij} = 1$ if the nodes are connected. Specifically, we randomly generated 100 graphs of $n = 5$ nodes according to the Erdős-Rényi model [55], such that each graph G is chosen uniformly at random from the set of all graphs of 5 nodes. For each graph and for different values of p we ran 10 instances of the parameter optimization, and we selected the run that achieved the smallest energy. At each optimization step the cost was estimated with 1000 shots.

To analyze the performance we present in Fig. 3(a) the

average approximation ratio when training the QAOA in the presence and absence of noise. The approximation ratio is defined as the lowest energy obtained via optimizing divided by the exact ground state energy of H_P . First, we note that when training in the absence of noise, the approximation ratio increases with circuit depth. However, when training in the presence of noise the performance decreases for $p > 4$. This result is in accordance with Lemma 1 as the cost function value concentrates around $\text{Tr}[H_P] = 0$ as p increases. This concentration phenomenon can also be seen clearly in Fig. 3(b), where in fact we see evidence of exponential decay with p .

In addition we can see the effect of NIBPs, as Fig. 3(a) also depicts the value of the approximation ratio computed without noise (by utilizing the parameters obtained via noisy training). Note that evaluating the cost in a noise-free setting has practical meaning, since the classicality of the Hamiltonian allows one to compute the cost on a (noise-free) classical computer, after training the parameters. For $p > 4$ this approximation ratio decreases, meaning that as p becomes larger it becomes increasingly hard to find a minimizing direction to navigate through the cost function landscape. Moreover, the effect of NIBPs is evident in Fig. 3(c) where we depict the average absolute value of the largest cost function partial derivative (i.e., $\max_{lm} |\partial_{lm} \tilde{C}|$). This plot shows an exponential decay with p of the partial derivative in accordance with Theorem 1.

The previous results show that training the QAOA in the presence of a realistic noise model significantly affects the performance, particularly as p increases beyond a threshold value ($p = 4$ in this case). The concentration of cost and the NIPB phenomenon are both clearly visible in our data, and they prevent us from obtaining large approximation ratios. Hence, noise appears to be a crucial factor to account for when attempting to understand the performance of QAOA.

III. Discussion

The success of NISQ computing largely depends on the scalability of Variational Quantum Algorithms (VQAs), which are widely viewed as the best hope for near-term quantum advantage for various applications. Only a small handful of works have analytically studied VQA scalability, and there is even less known about the impact of noise on their scaling. Our work represents a major breakthrough in understanding the effect of local noise on VQA scalability. We rigorously prove two important and closely related phenomena: the exponential concentration of the cost function in Lemma 1 and the exponential vanishing of the gradient in Theorem 1. We refer to the latter as a Noise-Induced Barren Plateau (NIPB). Like noise-free barren plateaus, NIPBs require the precision and hence the algorithmic complexity to scale exponentially with the problem size. Thus, avoiding NIPBs is necessary for a VQA to have any hope of exponential

quantum speedup.

On the other hand, NIBPs are conceptually different from noise-free barren plateaus [26–28]. The latter are due to random parameter initialization and hence can be addressed by pre-training, correlating parameters, and other strategies [29–32]. In contrast, NIBPs hold for every point on the cost function landscape. Hence, pre-training and other similar strategies do not avoid NIBPs, and we explicitly demonstrate this for the parameter correlation strategy in Remark 1. At the moment, the only strategies we are aware of for avoiding NIBPs are: (1) reducing the hardware noise level, or (2) improving the design of variational ansatzes such that their circuit depth scales more weakly with n . Our work provides quantitative guidance for how to develop these strategies. For example, Eq. (14) gives a condition on the ansatz circuit depth that must be avoided to prevent NIBPs.

An elegant feature of our work is its generality, as our results apply to a wide range of VQAs and ansatzes. This includes the two most popular ansatzes, QAOA for optimization and UCC for chemistry, which Corollaries 2 and 3 treat, respectively. In recent times, QAQA, UCC, and other physically motivated ansatzes have been touted as the potential solution to trainability issues due to (noise-free) barren plateaus, while Hardware Efficient ansatzes, which minimize circuit depth, have been regarded as problematic. Our work swings the pendulum in the other direction: any additional circuit depth that an ansatz incorporates (regardless of whether it is physically motivated) will hurt trainability and potentially lead to a NIBP. This suggests that Hardware Efficient ansatzes are in fact worth exploring further, provided one has an appropriate strategy to avoid noise-free barren plateaus. This claim is supported by recent state-of-the-art implementations for optimization [43] and chemistry [42] using such ansatzes.

We believe our work has particular relevance to optimization. For combinatorial optimization problems, such as MaxCut on 3-regular graphs, the compilation of a single instance of the problem unitary $e^{-i\gamma H_P}$ requires an $\Omega(n)$ -depth circuit [43]. Therefore, for a constant number of rounds p of the QAOA, the circuit depth grows at least linearly with n . From Theorem 1, it follows that NIBPs can occur for practical QAOA problems for sufficiently high noise values, even for constant number of rounds. Furthermore, assuming the aforementioned linear compilation overhead, NIBPs are guaranteed (asymptotically) if p grows in n . Such growth has been shown to be necessary in certain instances of MaxCut [45] as well as for other optimization problems [17, 48], and hence NIBPs are especially relevant in these cases.

While it is well known that decoherence ultimately limits the depth of quantum circuits in the NISQ era, there was an interesting open question (prior to our work) as to whether one could still train the parameters of a variational ansatz in the high decoherence limit. This question was especially important for VQAs for optimization, compiling, and linear systems, which are applications

that do not require accurate estimation of cost functions on the quantum computer. Our work essentially provides a negative answer to this question. Naturally, important future work will involve extending our results to more general (e.g., non-unital) noise models, and numerically testing the tightness of our bounds. Moreover, our work emphasizes the importance of short-depth variational ansatzes. Hence a crucial research direction for the success of VQAs will be the development of methods to reduce ansatz depth.

IV. Methods

A. Special Cases of Our Ansatz

Here we discuss how the the QAOA, the Hardware Efficient ansatz, and the UCC ansatz fit into the general framework of Section II A.

1. Quantum Alternating Operator Ansatz

The QAOA can be understood as a discretized adiabatic transformation where the goal is to prepare the ground state of a given Hamiltonian H_P . The order p of the Trotterization determines the solution precision and the circuit depth. Given a initial state $|s\rangle$, usually the linear superposition of all elements of the computational basis $|s\rangle = |+\rangle^{\otimes n}$, the ansatz corresponds to the sequential application of two unitaries $U_P(\gamma_l) = e^{-i\gamma_l H_P}$ and $U_M(\beta_l) = e^{-i\beta_l H_M}$. These alternating unitaries are usually known as the problem and mixer unitary, respectively. Here $\gamma = \{\gamma_k\}_{l=1}^L$ and $\beta = \{\beta_k\}_{l=1}^L$ are vectors of variational parameters which determine how long each unitary is applied and which must be optimized to minimize the cost function C , defined as the expectation value

$$C = \langle \gamma, \beta | H_P | \gamma, \beta \rangle = \text{Tr}[H_P | \gamma, \beta \rangle \langle \gamma, \beta |], \quad (23)$$

where $|\gamma, \beta\rangle = U(\gamma, \beta)|s\rangle$ is the QAOA variational state, and where $U(\gamma, \beta)$ is given by (5). In Fig. 4(a) we depict the circuit description of a QAOA ansatz for a specific Hamiltonian where $k_P = 6$.

2. Hardware Efficient Ansatz

The goal of the Hardware Efficient ansatz is to reduce the gate overhead (and hence the circuit depth) which arises when implementing a general unitary as in (3). Hence, when employing a specific quantum hardware the parametrized gates $e^{-i\theta_{lm} H_{lm}}$ and the unparametrized gates W_{lm} are taken from a gate alphabet composed of native gates to that hardware. Figure 4(b) shows an example of a Hardware Efficient ansatz where the gate alphabet is composed of rotations around the y axis and of CNOTs.

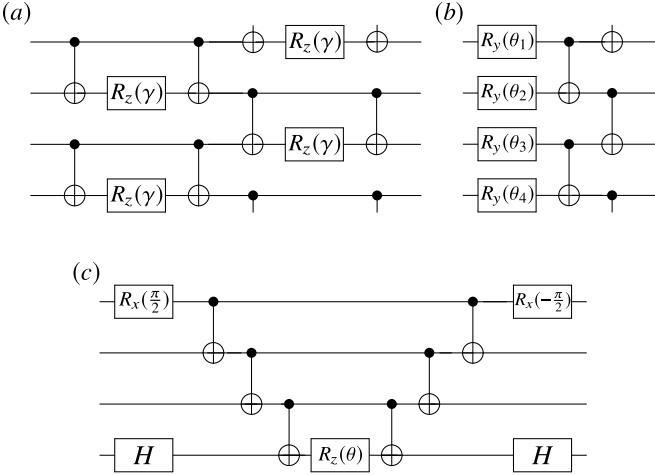


FIG. 4. **Special cases of our general ansatz.** (a) QAOA problem unitary $e^{-i\gamma H_P}$ for the ring-of-disagrees MaxCut problem, with Hamiltonian $H_P = \frac{1}{2} \sum_j Z_j Z_{j+1}$. (b) Hardware Efficient ansatz composed of CNOTs and single qubit rotations around the y -axis $R_y(\theta)$. (c) Unitary for the exponential $e^{-i\theta Y_1 Z_2 Z_3 X_4}$. This type of circuit is a representative component of the UCC ansatz.

3. Unitary Coupled Cluster Ansatz

This ansatz is employed to estimate the ground state energy of the molecular Hamiltonian. In the second quantization, and within the Born-Oppenheimer approximation, the molecular Hamiltonian of a system of M_e electrons can be expressed as: $H = \sum_{pq} h_{pq} a_p^\dagger a_q + \frac{1}{2} \sum_{pqrs} h_{pqrs} a_p^\dagger a_q^\dagger a_r a_s$, where $\{a_p^\dagger\}$ ($\{a_q\}$) are Fermionic creation (annihilation) operators. Here, h_{pq} and h_{pqrs} respectively correspond to the so-called one- and two-electron integrals [38, 49]. The ground state energy of H can be estimated with the VQE algorithm by preparing a reference state, normally taken to be the Hartree-Fock (HF) mean-field state $|\psi_0\rangle$, and acting on it with a parametrized UCC ansatz.

The action of a UCC ansatz with single (T_1) and double (T_2) excitations is given by $|\psi\rangle = \exp(T - T^\dagger)|\psi_0\rangle$, where $T = T_1 + T_2$, and where

$$T_1 = \sum_{\substack{i \in \text{occ} \\ a \in \text{vir}}} t_i^a a_a^\dagger a_i, \quad T_2 = \sum_{\substack{i,j \in \text{occ} \\ a,b \in \text{vir}}} t_{i,j}^{a,b} a_a^\dagger a_b^\dagger a_j a_i. \quad (24)$$

Here the i and j indices range over “occupied” orbitals whereas the a and b indices range over “virtual” orbitals [38, 49]. The coefficients t_i^a and $t_{i,j}^{a,b}$ are called coupled cluster amplitudes. For simplicity, we denote these amplitudes $\{t_i^a, t_{i,j}^{a,b}\}$ as $\{\theta_{lm}\}$. Similarly, by denoting the excitation operators $\{a_a^\dagger a_i, a_a^\dagger a_b^\dagger a_j a_i\}$ as $\{\tau_{lm}\}$, the UCC ansatz can be written in a compact form as $U(\theta) = e^{\sum_{lm} \theta_{lm} (\tau_{lm} - \tau_{lm}^\dagger)}$. In order to implement $U(\theta)$ one maps the fermionic operators to spin operators by means of the Jordan-Wigner or the Bravyi-Kitaev trans-

formations [51, 52], which allows us to write $(\tau_{lm} - \tau_{lm}^\dagger) = i \sum_i \mu_{lm}^i \sigma_n^i$. Then, from a first-order Trotterization we get (6). Here, $\mu_{lm}^i \in \{0, \pm 1\}$. In Fig. 4(c) we depict the circuit description of a representative component of the UCC ansatz.

B. Proof of Theorem 1

Here we outline the proof for our main result on Noise-Induced Barren Plateaus. We refer the reader to the Supplementary Information for additional details. We note that Lemma 1 and Remark 1 follow from similar steps and their proofs are also detailed in the Supplementary Information. Moreover, we remark that Corollaries 1, 2, and 3 follow in a straightforward manner from a direct application of Theorem 1 and Remark 1.

Before providing a sketch of our proof let us introduce some preliminary results that will be useful. Given an n -qubit operator Λ , one can always consider its expansion in the Pauli basis: $\Lambda = \frac{1}{2^n} (\lambda_0 \mathbb{1}^{\otimes n} + \boldsymbol{\lambda} \cdot \boldsymbol{\sigma}_n)$. Note that here we redefine the vector of Pauli strings $\boldsymbol{\sigma}_n$ as a vector of length $4^n - 1$ which excludes $\mathbb{1}^{\otimes n}$. First, let us analyze how a unitary channel affects $\boldsymbol{\lambda}$. Note that since $\text{Tr}[\Lambda] = \lambda_0$, and $\text{Tr}[\Lambda^2] = \frac{1}{2^n} (\lambda_0^2 + \|\boldsymbol{\lambda}\|_2^2)$ are invariant under unitary transformations, then $\|\boldsymbol{\lambda}\|_2$ is also invariant under unitary transformations. Second, we investigate how $\boldsymbol{\lambda}$ is affected under local Pauli noise, as defined in Eq. (7). Denote $\boldsymbol{\lambda}^{(l)}$ as the vector obtained after l applications of noise and unitary channels. The action of the next noisy channel is to map the elements of $\boldsymbol{\lambda}^{(l)}$ as $\lambda_i^{(l)} \xrightarrow{\mathcal{N}} q_X^{x(i)} q_Y^{y(i)} q_Z^{z(i)} \lambda_i^{(l)}$ where $x(i)$, $y(i)$, and $z(i)$ respectively denote the number of X , Y , and Z operators in the i -th Pauli string. Recall that $q = \max\{|q_X|, |q_Y|, |q_Z|\}$. Since $x(i) + y(i) + z(i) \geq 1$, the inequality $\|\boldsymbol{\lambda}^{(l+1)}\|_2 \leq q \|\boldsymbol{\lambda}^{(l)}\|_2$ always holds, and therefore we have

$$\|\boldsymbol{\lambda}^{(k)}\|_2 \leq q^{k-l} \|\boldsymbol{\lambda}^{(l)}\|_2 \quad (25)$$

for any choice of layers $1 \leq l \leq k \leq L$.

Using the above, we can now provide a sketch of the proof of Theorem 1. First, let us define $\rho_0 = \rho$ as the input state of the circuit and further define ρ_l as the state obtained after the application of the l -th unitary of the ansatz, i.e. $\rho_l = (\mathcal{U}_l \circ \mathcal{N} \circ \dots \circ \mathcal{U}_1 \circ \mathcal{N})(\rho)$. This state can be written in the Pauli representation as

$$\rho_l = \frac{1}{2^n} (\mathbb{1}^{\otimes n} + \boldsymbol{a}^{(l)} \cdot \boldsymbol{\sigma}_n), \quad (26)$$

where $\boldsymbol{a}^{(l)} \in \mathbb{R}^n$. From Eq. (25) it follows that $\|\boldsymbol{a}^{(l)}\|_2 \leq q^l \|\boldsymbol{a}^{(0)}\|_2$. Moreover, if the input state is pure, we have $\|\boldsymbol{a}^{(0)}\|_2^2 = (2^n - 1)$.

In order to analyze the partial derivative of the cost function $\partial_{lm} \tilde{C} = \text{Tr} [O \partial_{lm} \rho_L]$ we first note that ρ_L can be expressed as

$$\rho_L = (\mathcal{W}_a \circ \mathcal{W}_b)(\rho_0) = \mathcal{W}_a(\bar{\rho}_l), \quad (27)$$

where

$$\mathcal{W}_a = \mathcal{N} \circ \mathcal{U}_L \circ \cdots \circ \mathcal{U}_{l+1} \circ \mathcal{N} \circ \mathcal{U}_m^+, \quad (28)$$

$$\mathcal{W}_b = \mathcal{U}_m^- \circ \mathcal{N} \circ \mathcal{U}_{l-1} \circ \cdots \circ \mathcal{N} \circ \mathcal{U}_1 \circ \mathcal{N}, \quad (29)$$

and where \mathcal{U}_m^\pm are channels that implement the unitaries $U_m^- = \prod_{s \leq m} e^{-i\theta_{ls} H_{ls}}$ and $U_m^+ = \prod_{s > m} e^{-i\theta_{ls} H_{ls}}$ such that $U_l = U_m^+ \cdot U_m^-$. For simplicity of notation here we have omitted the parameter dependence on the unitary channels. Additionally, we have introduced the notation $\bar{\rho}_l = \mathcal{W}_b(\rho_0)$ and it is straightforward to show that

$$\partial_{lm} \bar{\rho}_l = -i[H_{lm}, \bar{\rho}_l]. \quad (30)$$

In the Pauli basis we have $\partial_{lm} \bar{\rho}_l = \frac{1}{2^n} \mathbf{g}^{(l)} \cdot \boldsymbol{\sigma}_n$, where we note that no identity is present in the expansion as $\partial_{lm} \bar{\rho}_l$ is a traceless operator. Hence, we have that $\text{Tr}[\partial_{lm} \bar{\rho}_l]^2 = \frac{1}{2^n} \|\mathbf{g}^{(l)}\|_2^2$. Moreover, the following chain of equalities always holds

$$\begin{aligned} \text{Tr}[\partial_{lm} \bar{\rho}_l]^2 &= -\text{Tr}\left[\left[H_{lm}, \bar{\rho}_l\right]^2\right] \\ &= 2\text{Tr}\left[H_{lm}^2 \bar{\rho}_l^2\right] - 2\text{Tr}\left[H_{lm} \bar{\rho}_l H_{lm} \bar{\rho}_l\right] \\ &\leq 2 \cdot \frac{1}{2^n} N_{lm}^2 \|\boldsymbol{\eta}_{lm}\|_\infty^2 \|\mathbf{a}^{(l)}\|_2^2 \end{aligned} \quad (31)$$

where the inequality comes from expanding each term in terms of Pauli operators and using the fact that $H_{lm}^2 \leq N_{lm}^2 \|\boldsymbol{\eta}_{lm}\|_\infty^2 \mathbb{1}^{\otimes n}$. Note that Eq. (31) provides an upper bound for $\|\mathbf{g}^{(l)}\|_2$ in terms of $\|\mathbf{a}^{(l)}\|_2$ since this equation can be written as $\|\mathbf{g}^{(l)}\|_2^2 \leq 2N_{lm}^2 \|\boldsymbol{\eta}_{lm}\|_\infty^2 q^{2L+2}(2^n - 1)$. Finally, using the triangle inequality and the hierarchy of p -norms we obtain

$$|\partial_{lm} \tilde{C}| = |\text{Tr}[\partial_{lm} \rho_L O]| \quad (32)$$

$$\leq \sqrt{2} N_{lm} N_O \|\boldsymbol{\eta}_{lm}\|_\infty \|\boldsymbol{\omega}\|_\infty q^{L+1} \sqrt{2^n - 1}, \quad (33)$$

where we can use the fact that $(2^n - 1) \leq 2^n$ to obtain our main result in Eqs. (11)–(12).

C. Proof of Proposition 1

Here we sketch the proof of Proposition 1, with additional details being presented in the Supplementary Information.

Here we model measurement noise as a tensor product of independent local classical bit-flip channels, which mathematically corresponds to modifying the local POVM elements $P_0 = |0\rangle\langle 0|$ and $P_1 = |1\rangle\langle 1|$ as follows:

$$P_0 = |0\rangle\langle 0| \rightarrow \tilde{P}_0 = \frac{1+q_M}{2} |0\rangle\langle 0| + \frac{1-q_M}{2} |1\rangle\langle 1| \quad (34)$$

$$P_1 = |1\rangle\langle 1| \rightarrow \tilde{P}_1 = \frac{1-q_M}{2} |0\rangle\langle 0| + \frac{1+q_M}{2} |1\rangle\langle 1|. \quad (35)$$

In turn, it follows that one can also model this measurement noise as a tensor product of local depolarizing channels with depolarizing probability $1 \geq (1-q_M)/2 \geq 0$,

which we indicate by \mathcal{N}_M . The channel is applied directly to the measurement operator such that $\mathcal{N}_M(O) = \sum_i \omega^i \mathcal{N}_M(\sigma_n^i) = \tilde{\boldsymbol{\omega}} \cdot \boldsymbol{\sigma}_n$. Here $\tilde{\boldsymbol{\omega}}$ is a vector of coefficients $\tilde{\omega}^i = q_M^{w(i)} \omega^i$, where $w(i) = x(i) + y(i) + z(i)$ is the weight of the Pauli string. Here we recall that we have respectively defined $x(i)$, $y(i)$, $z(i)$ as the number of Pauli operators X , Y , and Z in the i -th Pauli string.

Let us first focus on the partial derivative of the cost. In the presence of measurement noise we then have

$$\partial_{lm} \tilde{C} = \frac{1}{2^n} \text{Tr} \left[(\tilde{\boldsymbol{\omega}} \cdot \boldsymbol{\sigma}_n) (\mathbf{g}^{(L)} \cdot \boldsymbol{\sigma}_n) \right] \quad (36)$$

$$= \tilde{\boldsymbol{\omega}} \cdot \mathbf{g}^{(L)}. \quad (37)$$

Which means that $|\partial_{lm} \tilde{C}| = |\tilde{\boldsymbol{\omega}} \cdot \mathbf{g}^{(L)}|$. We then examine the inner product in an element-wise fashion:

$$|\tilde{\boldsymbol{\omega}} \cdot \mathbf{g}^{(L)}| \leq \sum_i |\tilde{\omega}_i| |g_i^{(L)}| \leq \sum_i q_M^{w(i)} |\omega_i| |g_i^{(L)}|. \quad (38)$$

Therefore, defining $w = \min_i w(i)$ as the minimum weight of the Pauli strings in the decomposition of O , we have that $q_M^{w(i)} \leq q_M^w$, and hence we can replace $q_M^{w(i)}$ with q_M^w for each term in the sum. This gives an extra locality-dependent factor in the bound on the partial derivative:

$$|\partial_{lm} \tilde{C}| \leq q_M^w F(n). \quad (39)$$

An analogous reasoning leads to the following result for the concentration of the cost function:

$$\left| \tilde{C} - \frac{1}{2^n} \text{Tr} O \right| \leq q_M^w G(n). \quad (40)$$

D. Details of Numerical Implementations

The noise model employed in our numerical simulations was obtained by performing one- and two-qubit gate-set tomography [56, 57] on the five-qubit IBM Q Ourense superconducting qubit device. The process matrices for each gate native to the device's alphabet, and the state preparation and measurement noise are described in Ref. [58, Appendix B]. In addition, the optimization for the MaxCut problems was performed using an optimizer based on the Nelder-Mead simplex method.

V. ACKNOWLEDGEMENTS

Research presented in this article was supported by the Laboratory Directed Research and Development program of Los Alamos National Laboratory under project number 20190065DR. SW and EF acknowledge support from the U.S. Department of Energy (DOE) through a quantum computing program sponsored by the LANL Information Science & Technology Institute. MC and AS

were also supported by the Center for Nonlinear Studies at LANL. PJC also acknowledges support from the LANL ASC Beyond Moore's Law project. LC and PJC were also supported by the U.S. Department of Energy

(DOE), Office of Science, Office of Advanced Scientific Computing Research, under the Quantum Computing Applications Team (QCAT) program.

[1] J. Preskill, "Quantum computing in the NISQ era and beyond," *Quantum* **2**, 79 (2018).

[2] Jarrod R McClean, Jonathan Romero, Ryan Babbush, and Alán Aspuru-Guzik, "The theory of variational hybrid quantum-classical algorithms," *New Journal of Physics* **18**, 023023 (2016).

[3] A. Peruzzo, J. McClean, P. Shadbolt, M.-H. Yung, X.-Q. Zhou, P. J. Love, A. Aspuru-Guzik, and J. L. O'Brien, "A variational eigenvalue solver on a photonic quantum processor," *Nature Communications* **5**, 4213 (2014).

[4] Bela Bauer, Dave Wecker, Andrew J Millis, Matthew B Hastings, and Matthias Troyer, "Hybrid quantum-classical approach to correlated materials," *Physical Review X* **6**, 031045 (2016).

[5] Tyson Jones, Suguru Endo, Sam McArdle, Xiao Yuan, and Simon C Benjamin, "Variational quantum algorithms for discovering hamiltonian spectra," *Physical Review A* **99**, 062304 (2019).

[6] Ying Li and Simon C Benjamin, "Efficient variational quantum simulator incorporating active error minimization," *Physical Review X* **7**, 021050 (2017).

[7] Cristina Cirstoiu, Zoe Holmes, Joseph Iosue, Lukasz Cincio, Patrick J Coles, and Andrew Sornborger, "Variational fast forwarding for quantum simulation beyond the coherence time," *arXiv preprint arXiv:1910.04292* (2019).

[8] K. Heya, K. M. Nakanishi, K. Mitarai, and K. Fujii, "Subspace variational quantum simulator," *arXiv:1904.08566* [quant-ph].

[9] Xiao Yuan, Suguru Endo, Qi Zhao, Ying Li, and Simon C Benjamin, "Theory of variational quantum simulation," *Quantum* **3**, 191 (2019).

[10] E. Farhi, J. Goldstone, and S. Gutmann, "A quantum approximate optimization algorithm," *arXiv:1411.4028* [quant-ph].

[11] Z. Wang, S. Hadfield, Z. Jiang, and E. G. Rieffel, "Quantum approximate optimization algorithm for MaxCut: A fermionic view," *Phys. Rev. A* **97**, 022304 (2018).

[12] G. E. Crooks, "Performance of the quantum approximate optimization algorithm on the maximum cut problem," *arXiv:1811.08419* [quant-ph].

[13] Stuart Hadfield, Zhihui Wang, Bryan O'Gorman, Eleanor G Rieffel, Davide Venturelli, and Rupak Biswas, "From the quantum approximate optimization algorithm to a quantum alternating operator ansatz," *Algorithms* **12**, 34 (2019).

[14] Carlos Bravo-Prieto, Ryan LaRose, M. Cerezo, Yigit Subasi, Lukasz Cincio, and Patrick J. Coles, "Variational quantum linear solver: A hybrid algorithm for linear systems," *arXiv:1909.05820* (2019).

[15] X. Xu, J. Sun, S. Endo, Y. Li, S. C. Benjamin, and X. Yuan, "Variational algorithms for linear algebra," *arXiv:1909.03898* [quant-ph].

[16] Bálint Koczor, Suguru Endo, Tyson Jones, Yuichiro Matsuzaki, and Simon C Benjamin, "Variational-state quantum metrology," *arXiv preprint arXiv:1908.08904* (2019).

[17] Eric Anschuetz, Jonathan Olson, Alán Aspuru-Guzik, and Yudong Cao, "Variational quantum factoring," in *Quantum Technology and Optimization Problems*, edited by Sebastian Feld and Claudia Linnhoff-Popien (Springer International Publishing, Cham, 2019) pp. 74–85.

[18] S. Khatri, R. LaRose, A. Poremba, L. Cincio, A. T. Sornborger, and P. J. Coles, "Quantum-assisted quantum compiling," *Quantum* **3**, 140 (2019).

[19] Kunal Sharma, Sumeet Khatri, Marco Cerezo, and Patrick Coles, "Noise resilience of variational quantum compiling," *New Journal of Physics* (2020).

[20] T. Jones and S. C Benjamin, "Quantum compilation and circuit optimisation via energy dissipation," *arXiv:1811.03147* [quant-ph].

[21] A. Arrasmith, L. Cincio, A. T. Sornborger, W. H. Zurek, and P. J. Coles, "Variational consistent histories as a hybrid algorithm for quantum foundations," *Nature communications* **10**, 3438 (2019).

[22] Marco Cerezo, Alexander Poremba, Lukasz Cincio, and Patrick J Coles, "Variational quantum fidelity estimation," *Quantum* **4**, 248 (2020).

[23] M Cerezo, Kunal Sharma, Andrew Arrasmith, and Patrick J Coles, "Variational quantum state eigensolver," *arXiv preprint arXiv:2004.01372* (2020).

[24] Ryan LaRose, Arkin Tikku, Étude OâŽNeel-Judy, Lukasz Cincio, and Patrick J Coles, "Variational quantum state diagonalization," *npj Quantum Information* **5**, 1–10 (2019).

[25] Guillaume Verdon, Jacob Marks, Sasha Nanda, Stefan Leichenauer, and Jack Hidary, "Quantum hamiltonian-based models and the variational quantum thermalizer algorithm," *arXiv preprint arXiv:1910.02071* (2019).

[26] Jarrod R McClean, Sergio Boixo, Vadim N Smelyanskiy, Ryan Babbush, and Hartmut Neven, "Barren plateaus in quantum neural network training landscapes," *Nature communications* **9**, 4812 (2018).

[27] Kunal Sharma, M Cerezo, Lukasz Cincio, and Patrick J Coles, "Trainability of dissipative perceptron-based quantum neural networks," *arXiv preprint arXiv:2005.12458* (2020).

[28] M Cerezo, Akira Sone, Tyler Volkoff, Lukasz Cincio, and Patrick J Coles, "Cost-function-dependent barren plateaus in shallow quantum neural networks," *arXiv preprint arXiv:2001.00550* (2020).

[29] Tyler Volkoff and Patrick J Coles, "Large gradients via correlation in random parameterized quantum circuits," *arXiv preprint arXiv:2005.12200* (2020).

[30] Guillaume Verdon, Michael Broughton, Jarrod R McClean, Kevin J Sung, Ryan Babbush, Zhang Jiang, Hartmut Neven, and Masoud Mohseni, "Learning to learn with quantum neural networks via classical neural networks," *arXiv preprint arXiv:1907.05415* (2019).

[31] Edward Grant, Leonard Wossnig, Mateusz Ostaszewski, and Marcello Benedetti, “An initialization strategy for addressing barren plateaus in parametrized quantum circuits,” *Quantum* **3**, 214 (2019).

[32] Andrea Skolik, Jarrod R McClean, Masoud Mohseni, Patrick van der Smagt, and Martin Leib, “Layerwise learning for quantum neural networks,” *arXiv preprint arXiv:2006.14904* (2020).

[33] Cheng Xue, Zhao-Yun Chen, Yu-Chun Wu, and Guo-Ping Guo, “Effects of quantum noise on quantum approximate optimization algorithm,” *arXiv preprint arXiv:1909.02196* (2019).

[34] Jeffrey Marshall, Filip Wudarski, Stuart Hadfield, and Tad Hogg, “Characterizing local noise in qaoa circuits,” *arXiv preprint arXiv:2002.11682* (2020).

[35] Laura Gentini, Alessandro Cuccoli, Stefano Pirandola, Paola Verrucchi, and Leonardo Banchi, “Noise-assisted variational hybrid quantum-classical optimization,” *arXiv preprint arXiv:1912.06744* (2019).

[36] Jonas M Kübler, Andrew Arrasmith, Lukasz Cincio, and Patrick J Coles, “An adaptive optimizer for measurement-frugal variational algorithms,” *Quantum* **4**, 263 (2020).

[37] Andrew Arrasmith, Lukasz Cincio, Rolando D Somma, and Patrick J Coles, “Operator sampling for shot-frugal optimization in variational algorithms,” *arXiv preprint arXiv:2004.06252* (2020).

[38] Yudong Cao, Jonathan Romero, Jonathan P Olson, Matthias Degroote, Peter D Johnson, Mária Kieferová, Ian D Kivlichan, Tim Menke, Borja Peropadre, Nicolas PD Sawaya, *et al.*, “Quantum chemistry in the age of quantum computing,” *Chemical reviews* **119**, 10856–10915 (2019).

[39] Rodney J Bartlett and Monika Musiał, “Coupled-cluster theory in quantum chemistry,” *Reviews of Modern Physics* **79**, 291 (2007).

[40] Joonho Lee, William J Huggins, Martin Head-Gordon, and K Birgitta Whaley, “Generalized unitary coupled cluster wave functions for quantum computation,” *Journal of chemical theory and computation* **15**, 311–324 (2018).

[41] A. Kandala, A. Mezzacapo, K. Temme, M. Takita, M. Brink, J. M. Chow, and J. M. Gambetta, “Hardware-efficient variational quantum eigensolver for small molecules and quantum magnets,” *Nature* **549**, 242 (2017).

[42] Frank Arute, Kunal Arya, *et al.*, “Hartree-fock on a superconducting qubit quantum computer,” *arXiv preprint arXiv:2004.04174* (2020).

[43] Frank Arute, Kunal Arya, *et al.*, “Quantum approximate optimization of non-planar graph problems on a planar superconducting processor,” *arXiv preprint arXiv:2004.04197* (2020).

[44] Bryan O’Gorman, William J Huggins, Eleanor G Rieffel, and K Birgitta Whaley, “Generalized swap networks for near-term quantum computing,” *arXiv preprint arXiv:1905.05118* (2019).

[45] Sergey Bravyi, Alexander Kliesch, Robert Koenig, and Eugene Tang, “Obstacles to state preparation and variational optimization from symmetry protection,” *arXiv preprint arXiv:1910.08980* (2019).

[46] Zhihui Wang, Stuart Hadfield, Zhang Jiang, and Eleanor G. Rieffel, “Quantum approximate optimization algorithm for maxcut: A fermionic view,” *Phys. Rev. A* **97**, 022304 (2018).

[47] Matthew B Hastings, “Classical and quantum bounded depth approximation algorithms,” *arXiv preprint arXiv:1905.07047* (2019).

[48] V. Akshay, H. Philathong, M. E. S. Morales, and J. D. Biamonte, “Reachability deficits in quantum approximate optimization,” *Phys. Rev. Lett.* **124**, 090504 (2020).

[49] Sam McArdle, Suguru Endo, Alan Aspuru-Guzik, Simon C Benjamin, and Xiao Yuan, “Quantum computational chemistry,” *Reviews of Modern Physics* **92**, 015003 (2020).

[50] Jonathan Romero, Ryan Babbush, Jarrod R McClean, Cornelius Hempel, Peter J Love, and Alán Aspuru-Guzik, “Strategies for quantum computing molecular energies using the unitary coupled cluster ansatz,” *Quantum Science and Technology* **4**, 014008 (2018).

[51] Gerardo Ortiz, James E Gubernatis, Emanuel Knill, and Raymond Laflamme, “Quantum algorithms for fermionic simulations,” *Physical Review A* **64**, 022319 (2001).

[52] Sergey B Bravyi and Alexei Yu Kitaev, “Fermionic quantum computation,” *Annals of Physics* **298**, 210–226 (2002).

[53] Marcel Nooijen, “Can the eigenstates of a many-body hamiltonian be represented exactly using a general two-body cluster expansion?” *Physical review letters* **84**, 2108 (2000).

[54] Dave Wecker, Matthew B Hastings, and Matthias Troyer, “Progress towards practical quantum variational algorithms,” *Physical Review A* **92**, 042303 (2015).

[55] P Erdos and A Renyi, “On random graphs i,” *Publ. math. debrecen* **6**, 18 (1959).

[56] Robin Blume-Kohout, John King Gamble, Erik Nielsen, Kenneth Rudinger, Jonathan Mizrahi, Kevin Fortier, and Peter Maunz, “Demonstration of qubit operations below a rigorous fault tolerance threshold with gate set tomography,” *Nature communications* **8**, 1–13 (2017).

[57] Erik Nielsen, Kenneth Rudinger, Timothy Proctor, Antonio Russo, Kevin Young, and Robin Blume-Kohout, “Probing quantum processor performance with pyGSTi,” *Quantum Science and Technology* **5**, 044002 (2020).

[58] Lukasz Cincio, Kenneth Rudinger, Mohan Sarovar, and Patrick J Coles, “Machine learning of noise-resilient quantum circuits,” *arXiv preprint arXiv:2007.01210* (2020).

[59] M. A. Nielsen and I. L. Chuang, *Quantum Computation and Quantum Information*, Cambridge University Press (2010).

[60] M. M. Wilde, *Quantum Information Theory*, 2nd ed. (Cambridge University Press, 2017).

Supplementary Information for Noise-Induced Barren Plateaus in Variational Quantum Algorithms

In this Supplementary Information we provide proofs for the main results of the manuscript “Noise-Induced Barren Plateaus in Variational Quantum Algorithms”. In Section A we first present some definitions and lemmas which will be useful in deriving our results. We point readers to [59, 60] for additional background. Then, in Section B we present a detailed proof of Theorem 1. Sections C and D respectively contain the proofs for Lemma 1, and Remark 1, while the proofs of Corollaries 2 and 3 are given in Sections E and F, respectively. Finally, the proof for Proposition 1 is detailed in Section G.

A. Preliminaries

1. Definitions

Pauli Expansion. Let us first recall that one can always expand H_{lm} and O in the Pauli basis as

$$H_{lm} = \sum_i \eta_{lm}^i \sigma_n^i = c_{lm}^0 \sigma_n^0 + \boldsymbol{\eta}_{lm} \cdot \boldsymbol{\sigma}_n, \quad (\text{A1})$$

$$O = \sum_i \omega^i \sigma_n^i = \omega^0 \sigma_n^0 + \boldsymbol{\omega} \cdot \boldsymbol{\sigma}_n. \quad (\text{A2})$$

where now $\sigma_n^i \in \{\mathbb{1}, X, Y, Z\}^{\otimes n} \setminus \{\mathbb{1}^{\otimes n}\}$ length- n Pauli strings. Here we remark that for the sake of simplicity we have made a subtle change in notation as now $\sigma_n^0 = \mathbb{1}^{\otimes n}$ is treated on a separate footing. With this notation, $\boldsymbol{\sigma}_n, \boldsymbol{\eta}_{lm}, \boldsymbol{\omega}$ are vectors of length $2^{2n} - 1$ and run over indices $i \in [4^n - 1]$. Moreover, we recall that we have defined $N_{lm} = |\boldsymbol{\eta}_{lm}|$, and $N_O = |\boldsymbol{\omega}|$ as the number of non-zero elements in each respective vector. Furthermore, note that we can always set $\omega^0 = 0$ and $\eta_{lm}^0 = 0$ for all lm . This does not lose us generality in our setting as a non-zero ω^0 corresponds to a trivial measurement, while a non-zero η_{lm}^0 simply leads to a different choice in the Hamiltonian normalization.

Vector Norms. In what follows we use the usual definitions of the p -norms such that $\|\mathbf{a}\|_\infty \equiv \max_i |a_i|$ is the largest element of vector \mathbf{a} and $\|\mathbf{a}\|_2 \equiv \sqrt{\sum_i |a_i|^2}$ is the Euclidean norm.

Setting for our analysis. As shown in Fig. 5 we break down the circuit into L unitaries preceded and followed by noisy channels acting on all qubits. Let ρ_0 and ρ_l respectively denote the input state and the state obtained after the l -th unitary. Let $\mathcal{N} = \mathcal{N}_1 \otimes \cdots \otimes \mathcal{N}_n$ denote the n -qubit noise channel. Then the noisy cost function \tilde{C} , defined as the expectation value of an operator O , can be represented as follows:

$$\tilde{C} = \text{Tr} \left[O (\mathcal{N} \circ \mathcal{U}_L(\boldsymbol{\theta}_L) \circ \mathcal{N} \circ \cdots \circ \mathcal{U}_2(\boldsymbol{\theta}_2) \circ \mathcal{N} \circ \mathcal{U}_1(\boldsymbol{\theta}_1) \circ \mathcal{N})(\rho_0) \right], \quad (\text{A3})$$

where the l -th unitary channel $\mathcal{U}_l(\boldsymbol{\theta}_l)$ implements the unitary operator

$$U_l(\boldsymbol{\theta}_l) = \prod_m e^{-i\theta_{lm} H_{lm}} W_{lm}. \quad (\text{A4})$$

Here we recall that $\boldsymbol{\theta}_l = \{\theta_{lm}\}$ are continuous parameters and W_{lm} denote unparameterized gates.

Noise model. We consider a noise model where local Pauli noise channels \mathcal{N}_j act on each qubit j before and after each unitary $U_l(\boldsymbol{\theta}_l)$. The action of \mathcal{N}_j on a local Pauli operator $\sigma \in \{X, Y, Z\}$ can be expressed as

$$\mathcal{N}_j(\sigma) = q_\sigma \sigma, \quad (\text{A5})$$

where $-1 < q_X, q_Y, q_Z < 1$. Here, we characterize the noise strength with a single parameter

$$q = \max\{|q_X|, |q_Y|, |q_Z|\}. \quad (\text{A6})$$

Representation of the quantum state. Here we will use the Pauli representation of an n qubit state

$$\rho = \frac{1}{2^n} \left(\mathbb{1}^{\otimes n} + \mathbf{a} \cdot \boldsymbol{\sigma}_n \right), \quad (\text{A7})$$

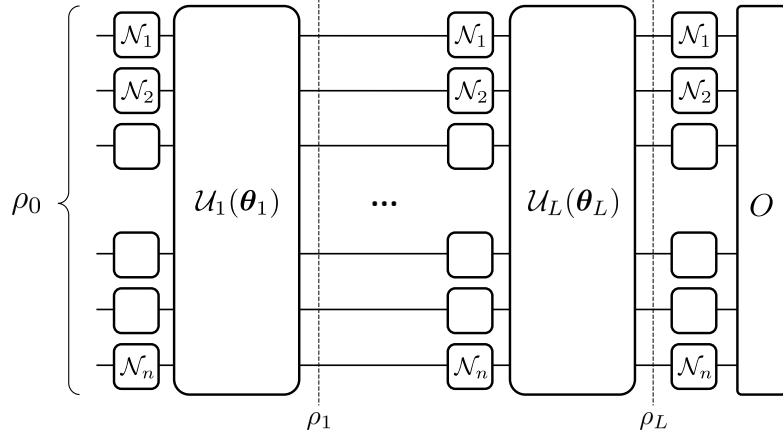


FIG. 5. Setting for our analysis. An n -qubit input state ρ_0 is sent through a variational ansatz $U(\theta)$ composed of L unitary layers $U_l(\theta_l)$ sequentially acting according to Eq. (A4). Here, \mathcal{U}_l denotes the quantum channel that implements the unitary $U_l(\theta_l)$. The parameters in the ansatz $\theta = \{\theta_l\}_{l=1}^L$ are trained to minimize a cost function that is expressed as the expectation value of an operator O as in Eq. (A3). We consider a noise model where local Pauli noise channels \mathcal{N}_j act on each qubit j before and after each unitary. We denote the state obtained after l applications of noise followed by unitary as ρ_l .

where $a_i = \langle \sigma_n^i \rangle = \text{Tr}[\rho \sigma_n^i]$. The state ρ can then be represented by a vector \mathbf{a} of length $(4^n - 1)$, with elements a_i , which we will refer to as the Pauli coefficients.

Recalling that ρ_l is the state obtained after the application of the l -th unitary, we employ the notation $a_i^{(l)}$ for its Pauli coefficients. That is, we explicitly write the output of layer l as

$$\rho_l = \frac{1}{2^n} (\mathbb{1}^{\otimes n} + \sum_{i=1}^{2^{2n}-1} a_i^{(l)} \sigma_n^i) = \frac{1}{2^n} (\mathbb{1}^{\otimes n} + \mathbf{a}^{(l)} \cdot \boldsymbol{\sigma}_n). \quad (\text{A8})$$

2. Useful Lemmas

Here we present and prove three supplementary lemmas which will be used in deriving our main results.

Supplementary Lemma 1. *Let Λ be an n -qubit operator whose Pauli basis decomposition is*

$$\Lambda = \frac{1}{2^n} (\lambda_0 \mathbb{1}^{\otimes n} + \boldsymbol{\lambda} \cdot \boldsymbol{\sigma}_n), \quad (\text{A9})$$

where $\lambda_0 \in \mathbb{R}$ and $\boldsymbol{\lambda} \in \mathbb{R}^{4^n-1}$. Then $\|\boldsymbol{\lambda}\|_2$ is invariant under unitary transformation $\Lambda \rightarrow U \Lambda U^\dagger$.

Proof. We note that $\text{Tr}[\Lambda]$ and $\text{Tr}[\Lambda^2]$ are respectively given by

$$\text{Tr}[\Lambda] = \lambda_0, \quad \text{Tr}[\Lambda^2] = \frac{1}{2^n} (\lambda_0^2 + \|\boldsymbol{\lambda}\|_2^2). \quad (\text{A10})$$

Since unitary operations preserve both quantities, then it follows that $\|\boldsymbol{\lambda}\|_2$ is also invariant under unitary transformation of Λ . \square

Supplementary Lemma 2. *Consider the quantum circuit as outlined in Fig. 5. Let ρ_k be the output state obtained after the action of the k -th unitary with Pauli decomposition given by (A8). Then the largest Pauli coefficient of ρ_k satisfies*

$$\|\mathbf{a}^{(k)}\|_\infty \leq \|\mathbf{a}^{(k)}\|_2 \leq q^{k-l} \|\mathbf{a}^{(l)}\|_2, \quad (\text{A11})$$

for any k, l such that $1 \leq l \leq k \leq L$.

Proof. As shown in the Supplementary Lemma 1, unitaries preserve the 2-norm of the generalized Bloch vector. Hence, we only need to consider the effect of $k - l$ layers of noise. The effect of a single layer of Pauli noise at layer l can be expressed as follows

$$a_i^{(l)} \xrightarrow{\mathcal{N}} q_X^{x(i)} q_Y^{y(i)} q_Z^{z(i)} a_i^{(l)}, \quad (\text{A12})$$

where $1 \leq x(i) + y(i) + z(i) \leq n$ is the number of non-identity terms in the i -th Pauli string. Applying the bound $x(i) + y(i) + z(i) \geq 1 \forall i$ and using Eq. (A6), we obtain

$$\|\mathbf{a}^{(k)}\|_2 \leq q \|\mathbf{a}^{(k-1)}\|_2. \quad (\text{A13})$$

Recursively using the same argument we get

$$\|\mathbf{a}^{(k)}\|_2 \leq q^{k-l} \|\mathbf{a}^{(l)}\|_2, \quad (\text{A14})$$

where $\mathbf{a}^{(0)}$ is the vector of Pauli coefficients for the input state ρ_0 . Finally, from the hierarchy of p -norms we have

$$\|\mathbf{a}^{(k)}\|_\infty \leq q^{k-l} \|\mathbf{a}^{(l)}\|_2. \quad (\text{A15})$$

□

Supplementary Lemma 3. *Consider the quantum circuit as outlined in Fig. 5, and assume that the input state is pure, i.e., $\rho_0 = |\psi^n\rangle\langle\psi^n|$. Then we have that*

$$\|\mathbf{a}^{(l)}\|_\infty \leq \|\mathbf{a}^{(l)}\|_2 \leq q^l (2^n - 1)^{1/2} \quad (\text{A16})$$

Proof. The purity of an n -qubit state ρ is given by

$$P(\rho) = \frac{1}{2^n} (1 + \|\mathbf{a}\|_2^2). \quad (\text{A17})$$

Since for a pure state, $P(\rho) = 1$, from Eq. (A17) it follows that $\|\mathbf{a}^{(0)}\|_2^2 = (2^n - 1)$. Invoking Eq. (A14), we get $\|\mathbf{a}^{(l)}\|_2 \leq q^l \|\mathbf{a}^{(0)}\|_2 = q^l (2^n - 1)^{1/2}$. □

B. Proof of Theorem 1

Here we provide the proof for our main result of Theorem 1, which we now recall for convinience.

Theorem 1 (Upper bound on the partial derivative). *Consider an L -layered ansatz as defined in Eq. (A4). Let θ_{lm} denote the trainable parameter corresponding to the Hamiltonian H_{lm} in the unitary $U_l(\theta_l)$ appearing in the ansatz. Suppose that local Pauli noise of the form in Eq. (A5) with noise parameter q acts before and after each layer as in Fig. 5. Then the following bound holds for the partial derivative of the noisy cost function*

$$|\partial_m \tilde{C}| \leq F(n), \quad (\text{B1})$$

where

$$F(n) = \sqrt{2} N_{lm} N_O \|\boldsymbol{\eta}_{lm}\|_\infty \|\boldsymbol{\omega}\|_\infty 2^{n/2} q^{L+1}, \quad (\text{B2})$$

and where $\boldsymbol{\eta}_{lm}$ and $\boldsymbol{\omega}$ are defined in Eq. (A1), as respective number of non-zero elements N_{lm} and N_O .

Proof. We write the overall channel that the state undergoes before measurement as

$$\mathcal{N} \circ \mathcal{U}_L(\boldsymbol{\theta}_L) \circ \cdots \circ \mathcal{N} \circ \mathcal{U}_2(\boldsymbol{\theta}_2) \circ \mathcal{N} \circ \mathcal{U}_1(\boldsymbol{\theta}_1) \circ \mathcal{N}(\cdot) = \mathcal{W}_a \circ \mathcal{W}_b(\cdot) \quad (\text{B3})$$

where

$$\mathcal{W}_b = \mathcal{U}_m^-(\boldsymbol{\theta}_l) \circ \mathcal{N} \circ \mathcal{U}_{l-1}(\boldsymbol{\theta}_{l-1}) \circ \cdots \circ \mathcal{N} \circ \mathcal{U}_1(\boldsymbol{\theta}_1) \circ \mathcal{N}, \quad (\text{B4})$$

$$\mathcal{W}_a = \mathcal{N} \circ \mathcal{U}_L(\boldsymbol{\theta}_L) \circ \cdots \circ \mathcal{U}_{l+1}(\boldsymbol{\theta}_{l+1}) \circ \mathcal{N} \circ \mathcal{U}_m^+(\boldsymbol{\theta}_l). \quad (\text{B5})$$

Here we define the unitary channels $\mathcal{U}_m^-(\boldsymbol{\theta}_l)$ and $\mathcal{U}_m^+(\boldsymbol{\theta}_l)$ that respectively correspond to the following unitaries:

$$U_m^-(\boldsymbol{\theta}_l) = \prod_{s=1}^m e^{-i\theta_{ls} H_{ls}}, \quad U_m^+(\boldsymbol{\theta}_l) = \prod_{s>m} e^{-i\theta_{ls} H_{ls}}. \quad (\text{B6})$$

For simplicity of notation let us denote $\partial_{lm} \tilde{C} = \partial_{\theta_{lm}} \tilde{C}$. Note that since

$$\partial_{lm} \tilde{C} = \text{Tr}[O \partial_{lm} \rho_L], \quad (\text{B7})$$

with

$$\partial_{lm} \rho_L = \partial_{lm} (\mathcal{W}_a \circ \mathcal{W}_b(\rho_0)) \quad (\text{B8})$$

$$= \mathcal{W}_a(\partial_{lm} \bar{\rho}_l), \quad (\text{B9})$$

where we denote $\bar{\rho}_l = \mathcal{W}_b(\rho_0)$. Then $\partial_{lm} \bar{\rho}_l$ can be simplified as follows:

$$\partial_{lm} \bar{\rho}_l = -i H_{lm} \bar{\rho}_l + i \bar{\rho}_l H_{lm} \quad (\text{B10})$$

$$= -i [H_{lm}, \bar{\rho}_l]. \quad (\text{B11})$$

Let $\mathbf{g}^{(l)}$ denote the vector in the Pauli representation of $\partial_{lm} \bar{\rho}_l$. Note that since $\partial_{lm} \bar{\rho}_l$ is a traceless operator, then its Pauli decomposition will not contain a term proportional to $\mathbb{1}^{\otimes n}$. Hence, we can write

$$\partial_{lm} \bar{\rho}_l = \frac{1}{2^n} \mathbf{g}^{(l)} \cdot \boldsymbol{\sigma}, \quad (\text{B12})$$

which leads to

$$\text{Tr}[|\partial_{lm} \bar{\rho}_l|^2] = \frac{1}{2^n} \|\mathbf{g}^{(l)}\|_2^2. \quad (\text{B13})$$

We now find a bound on $\text{Tr}[(\partial_{lm} \bar{\rho}_l)^2]$. By inserting the commutator in Eq. (B11) directly into the expression of $\text{Tr}[(\partial_{lm} \bar{\rho}_l)^2]$ we have that

$$\text{Tr}[|\partial_{lm} \bar{\rho}_l|^2] = -\text{Tr}[[H_{lm}, \bar{\rho}_l]^2] \quad (\text{B14})$$

$$= 2\text{Tr}[H_{lm}^2 \bar{\rho}_l^2] - 2\text{Tr}[H_{lm} \bar{\rho}_l H_{lm} \bar{\rho}_l] \quad (\text{B15})$$

where in Eq. (B14) we used the fact that $[H_{lm}, \bar{\rho}_l]^\dagger = -[H_{lm}, \bar{\rho}_l]$. The first term in Eq. (B15) can be written as follows

$$\text{Tr}[H_{lm}^2 \bar{\rho}_l^2] = \frac{1}{2^{2n}} \text{Tr} \left[\sum_a \eta_{lm}^a \sigma_n^a \sum_b \eta_{lm}^b \sigma_n^b (\mathbb{1}^{\otimes n} + \mathbf{a}^{(l)} \cdot \boldsymbol{\sigma}_n) (\mathbb{1}^{\otimes n} + \mathbf{a}^{(l)} \cdot \boldsymbol{\sigma}_n) \right] \quad (\text{B16})$$

$$= \frac{1}{2^{2n}} \sum_a \sum_b \text{Tr} \left[\eta_{lm}^a \eta_{lm}^b \sigma_n^a \sigma_n^b (\mathbb{1}^{\otimes n} + 2\mathbf{a}^{(l)} \cdot \boldsymbol{\sigma}_n + (\mathbf{a}^{(l)} \cdot \boldsymbol{\sigma}_n)^2) \right] \quad (\text{B17})$$

$$= \frac{1}{2^{2n}} \left(2^n N_{lm} \|\boldsymbol{\eta}_{lm}\|_\infty^2 + 2 \sum_a \sum_b \eta_{lm}^a \eta_{lm}^b \text{Tr}[\sigma_n^a \sigma_n^b (\mathbf{a}^{(l)} \cdot \boldsymbol{\sigma}_n)] + \text{Tr}[H_{lm}^2 (\mathbf{a}^{(l)} \cdot \boldsymbol{\sigma}_n)^2] \right) \quad (\text{B18})$$

$$\leq \frac{1}{2^{2n}} \left(2^n N_{lm} \|\boldsymbol{\eta}_{lm}\|_\infty^2 + 2 \sum_a \sum_b \eta_{lm}^a \eta_{lm}^b \text{Tr}[\sigma_n^a \sigma_n^b (\mathbf{a}^{(l)} \cdot \boldsymbol{\sigma}_n)] + 2^n N_{lm}^2 \|\boldsymbol{\eta}_{lm}\|_\infty^2 \|\mathbf{a}^{(l)}\|_2^2 \right), \quad (\text{B19})$$

where the inequality follows from the fact that $H_{lm}^2 \leq N_{lm}^2 \|\boldsymbol{\eta}_{lm}\|_\infty^2 \mathbb{1}^{\otimes n}$. For the second term in Eq. (B15) we have

$$\text{Tr}[H_{lm} \bar{\rho}_l H_{lm} \bar{\rho}_l] = \frac{1}{2^{2n}} \text{Tr} \left[\eta_{lm}^a \sum_a \sigma_n^a (\mathbb{1}^{\otimes n} + \mathbf{a}^{(l)} \cdot \boldsymbol{\sigma}_n) \eta_{lm}^b \sum_b \sigma_n^b (\mathbb{1}^{\otimes n} + \mathbf{a}^{(l)} \cdot \boldsymbol{\sigma}_n) \right] \quad (\text{B20})$$

$$= \frac{1}{2^{2n}} \sum_a \sum_b \eta_{lm}^a \eta_{lm}^b \text{Tr} \left[\sigma_n^a \sigma_n^b + \sigma_n^a (\mathbf{a}^{(l)} \cdot \boldsymbol{\sigma}_n) \sigma_n^b + \sigma_n^a \sigma_n^b (\mathbf{a}^{(l)} \cdot \boldsymbol{\sigma}_n) + (\mathbf{a}^{(l)} \cdot \sigma_n^a \boldsymbol{\sigma}_n) (\mathbf{a}^{(l)} \cdot \sigma_n^b \boldsymbol{\sigma}_n) \right] \quad (\text{B21})$$

$$= \frac{1}{2^{2n}} \left(2^n N_{lm} \|\boldsymbol{\eta}_{lm}\|_\infty^2 + 2 \sum_a \sum_b \eta_{lm}^a \eta_{lm}^b \text{Tr}[\sigma_n^a \sigma_n^b (\mathbf{a}^{(l)} \cdot \boldsymbol{\sigma}_n)] + \text{Tr} \left[\left(\sum_a \eta_{lm}^a \mathbf{a}^{(l)} \cdot \sigma_n^a \boldsymbol{\sigma}_n \right)^2 \right] \right) \quad (\text{B22})$$

$$\geq \frac{1}{2^{2n}} \left(2^n N_{lm} \|\boldsymbol{\eta}_{lm}\|_\infty^2 + 2 \sum_a \sum_b \eta_{lm}^a \eta_{lm}^b \text{Tr}[\sigma_n^a \sigma_n^b (\mathbf{a}^{(l)} \cdot \boldsymbol{\sigma}_n)] \right). \quad (\text{B23})$$

Combining Eqs. (B19) and (B23) we can then write Eq. (B15) as

$$\mathrm{Tr}[(\partial_{lm} \bar{\rho}_l)^2] = 2\mathrm{Tr}\left[H_{lm}^2 \bar{\rho}_l^2\right] - 2\mathrm{Tr}\left[H_{lm} \bar{\rho}_l H_{lm} \bar{\rho}_l\right] \quad (\text{B24})$$

$$\leq 2 \cdot \frac{1}{2^n} N_{lm}^2 \|\boldsymbol{\eta}_{lm}\|_\infty^2 \|\mathbf{a}^{(l)}\|_2^2, \quad (\text{B25})$$

which implies that

$$\|\mathbf{g}^{(l)}\|_2^2 \leq 2N_{lm}^2 \|\boldsymbol{\eta}_{lm}\|_\infty^2 \|\mathbf{a}^{(l)}\|_2^2. \quad (\text{B26})$$

Let us denote $\mathbf{g}^{(L)}$ as the vector in the Pauli representation of $\partial_{lm} \rho_L = \mathcal{W}_a(\partial_{lm} \bar{\rho}_l)$. Consider the following chain of inequalities:

$$\|\mathbf{g}^{(L)}\|_\infty^2 \leq q^{2(L-k+1)} \|\mathbf{g}^{(l)}\|_2^2 \quad (\text{B27})$$

$$\leq q^{2(L-k+1)} \cdot 2N_{lm}^2 \|\boldsymbol{\eta}_{lm}\|_\infty^2 \|\mathbf{a}^{(l)}\|_2^2 \quad (\text{B28})$$

$$\leq q^{2(L-k+1)} \cdot 2N_{lm}^2 \|\boldsymbol{\eta}_{lm}\|_\infty^2 q^{2k} (2^n - 1) \quad (\text{B29})$$

$$= 2N_{lm}^2 \|\boldsymbol{\eta}_{lm}\|_\infty^2 q^{2L+2} (2^n - 1). \quad (\text{B30})$$

The first inequality comes from application of Supplementary Lemma 2 and accounting for the final noise channel. The second inequality follows from Eq. (B26). Finally, the third inequality follows from Supplementary Lemma 3.

Therefore, $|\partial_{lm} \tilde{C}|$ can be bounded as follows:

$$|\partial_{lm} \tilde{C}| = |\mathrm{Tr}[\partial_{lm} \rho_L O]| \quad (\text{B31})$$

$$= |\mathrm{Tr}[\partial_{lm} \rho_L \boldsymbol{\omega} \cdot \boldsymbol{\sigma}_n]| \quad (\text{B32})$$

$$= |\mathbf{g}^{(L)} \cdot \boldsymbol{\omega}| \quad (\text{B33})$$

$$\leq N_O \|\mathbf{g}^{(L)}\|_\infty \cdot \|\boldsymbol{\omega}\|_\infty \quad (\text{B34})$$

$$= \sqrt{2} N_{lm} N_O \|\boldsymbol{\eta}_{lm}\|_\infty \|\boldsymbol{\omega}\|_\infty q^{L+1} \sqrt{2^n - 1} \quad (\text{B35})$$

where in Eq. (B34) we have used the fact that $\omega^a \leq \|\boldsymbol{\omega}\|_\infty$ for all a . Finally, employing the bound $(2^n - 1) \leq 2^n$ leads to Eqs. (B1)–(B2) in Theorem 1. \square

C. Proof of Lemma 1

In this section, we provide a proof for Lemma 1. We note that this Lemma is derived by employing techniques similar to those used in deriving Theorem 1 in Section B.

Lemma 1 (Concentration of the cost function). *Consider an L layer ansatz of the form in Eq. (A4). Suppose that local Pauli noise of the form of Eq. (A5) with noise strength q acts before and after each layer as in Fig. 5. Then, for a cost function \tilde{C} of the form in Eq. (A3), the following bound holds*

$$\left| \tilde{C} - \frac{1}{2^n} \mathrm{Tr}[O] \right| \leq G(n) \quad (\text{C1})$$

where

$$G(n) = N_O \|\boldsymbol{\omega}\|_\infty 2^{n/2} q^{L+1}. \quad (\text{C2})$$

Here $\|\cdot\|_\infty$ is the infinity norm, $\boldsymbol{\omega}$ is defined in Eq. (A1) and $N_O = |\boldsymbol{\omega}|$ is the number of non-zero elements in the Pauli decomposition of O .

Proof. Using Eq. (A3), the noisy cost function can be represented as follows:

$$\tilde{C} = \mathrm{Tr}[O \mathcal{N}(\rho_L)] \quad (\text{C3})$$

$$= \frac{1}{2^n} (\mathrm{Tr}[O] + \mathrm{Tr}[O(\tilde{\mathbf{a}}^{(L+1)} \cdot \boldsymbol{\sigma}_n)]), \quad (\text{C4})$$

where we represented $\mathcal{N}(\rho_L)$ as $(\mathbb{1} + \tilde{\mathbf{a}}^{(L+1)} \cdot \boldsymbol{\sigma}_n)/2^n$. Then, we get

$$\left| \tilde{C} - \frac{1}{2^n} \text{Tr}[O] \right| = \frac{1}{2^n} \left| \text{Tr}[O(\tilde{\mathbf{a}}^{(L+1)} \cdot \boldsymbol{\sigma}_n)] \right| \quad (\text{C5})$$

$$= \frac{1}{2^n} \left| \text{Tr}[(\boldsymbol{\omega} \cdot \boldsymbol{\sigma}_n)(\tilde{\mathbf{a}}^{(L+1)} \cdot \boldsymbol{\sigma}_n)] \right| \quad (\text{C6})$$

$$= \boldsymbol{\omega} \cdot \tilde{\mathbf{a}}^{(L+1)} \quad (\text{C7})$$

$$\leq N_O \|\boldsymbol{\omega}\|_\infty \|\tilde{\mathbf{a}}^{(L+1)}\|_\infty \quad (\text{C8})$$

$$\leq N_O \|\boldsymbol{\omega}\|_\infty q^{L+1} (2^n - 1)^{1/2}, \quad (\text{C9})$$

where the last inequality follows from Supplementary Lemma 3. Finally, Lemma 1 follows from the bound $(2^n - 1) \leq 2^n$. \square

D. Proof of Remark 1

We here present an extension to Theorem 1 to the case when several parameters in the ansatz $U(\boldsymbol{\theta})$ are correlated. Here, by correlated, we mean they are equal to each other [29]. Note that this is in contrast to the previously analyzed cases where we assumed that all parameters $\{\theta_{lm}\}_{lm}$ are independent. Specifically, Remark 1 provides an upper bound on the partial derivative of the cost function with respect to a parameter that is degenerate in $\boldsymbol{\theta}$.

Remark 1 (Degenerate parameters). *Consider the ansatz defined in Eqs. (A4). Suppose there is a subset G_{st} of the set $\{\theta_{lm}\}$ in this ansatz such that G_{st} consists of b parameters that are degenerate:*

$$G_{st} = \{\theta_{lm} \mid \theta_{lm} = \theta_{st}\} \quad (\text{D1})$$

Here, θ_{st} denotes the parameter in G_{st} for which $N_{lm} \|\boldsymbol{\eta}_{lm}\|_\infty$ takes the largest value in the set. (θ_{st} can also be thought of as a reference parameter to which all other parameters are set equal in value.) Then the partial derivative of the noisy cost with respect to θ_{st} is bounded as

$$|\partial_{st} \tilde{C}| \leq \sqrt{2} b N_{st} N_O \|\boldsymbol{\eta}_{st}\|_\infty \|\boldsymbol{\omega}\|_\infty 2^{n/2} q^{L+1} \quad (\text{D2})$$

at all points in the cost landscape.

Proof. Using arguments similar to those in Section B, we get

$$|\partial_{st} \tilde{C}| = \sum_{\theta_{hg} \in G_{st}} |\text{Tr}[O \partial_{hg} \rho_L]| \quad (\text{D3})$$

$$\leq \sum_{\theta_{hg} \in G_{st}} \sqrt{2} N_{hg} N_O \|\boldsymbol{\eta}_{hg}\|_\infty \|\boldsymbol{\omega}\|_\infty 2^{n/2} q^{L+1} \quad (\text{D4})$$

where the inequality was obtained from Eq. (B35). Since there are b terms in the summation, we have

$$|\partial_{st} \tilde{C}| \leq \sqrt{2} b N_{st} N_O \|\boldsymbol{\eta}_{st}\|_\infty \|\boldsymbol{\omega}\|_\infty 2^{n/2} q^{L+1}. \quad (\text{D5})$$

\square

We note that the proof of Remark 1 can be trivially generalized to the case when the parameters in G_{st} are linear functions of the reference parameter.

E. Proof of Corollary 2

In this section we provide a proof of Corollary 2. We start by recalling that in the QAOA one sequentially alternates the action of two unitaries as

$$U(\boldsymbol{\gamma}, \boldsymbol{\beta}) = e^{-i\beta_p H_M} e^{-i\gamma_p H_P} \dots e^{-i\beta_1 H_M} e^{-i\gamma_1 H_P}, \quad (\text{E1})$$

where H_P and H_M are the so-called problem and mixer Hamiltonian, respectively. We define N_P (N_M) the number of terms in the Pauli decompositions of H_P (H_M).

Corollary 2 (Example: QAOA). *Consider the QAOA with $2p$ trainable parameters, as defined in Eq. (E1). Suppose that the implementation of unitaries corresponding to the problem Hamiltonian H_P and the mixer Hamiltonian H_M require k_P - and k_M -depth circuits, respectively. If local Pauli noise of the form in Eq. (A5) with noise parameter q acts before and after each layer of native gates, then we have*

$$|\partial_{\beta_l} \tilde{C}| \leq \sqrt{2} b_{l,P} N_P \|\boldsymbol{\eta}_P\|_\infty \|\boldsymbol{\omega}\|_\infty 2^{n/2} q^{(k_P+k_M)p+1}, \quad (\text{E2})$$

$$|\partial_{\gamma_l} \tilde{C}| \leq \sqrt{2} b_{l,M} N_P \|\boldsymbol{\eta}_M\|_\infty \|\boldsymbol{\omega}\|_\infty 2^{n/2} q^{(k_P+k_M)p+1} \quad (\text{E3})$$

for any choice of parameters β_l, γ_l , and where $O = H_P$ in Eq. (A2). Here $b_{l,P}$ and $b_{l,M}$ are respectively the number of native gates parameterized by β_l and γ_l according to the compilation.

Proof. We now treat each layer of native hardware gates as a unitary layer as in Fig. 5, which gives $L = (k_P + k_M)p$. In Eq. (D5) we have $N_{st} = 1$, $\|\boldsymbol{\eta}_{\beta_l}\|_\infty \leq \|\boldsymbol{\eta}_P\|_\infty$, $\|\boldsymbol{\eta}_{\gamma_l}\|_\infty \leq \|\boldsymbol{\eta}_M\|_\infty$, assuming Trotterization. Then Corollary 2 follows by invoking Remark 1. \square

F. Proof of Corollary 3

In this section we provide a proof for Corollary 3. We recall that the UCC ansatz can be expressed as

$$U(\boldsymbol{\theta}) = \prod_{lm} U_{lm}(\theta_{lm}) = \prod_{lm} e^{i\theta_{lm} \sum_k \mu_{lm}^k \sigma_n^k}, \quad (\text{F1})$$

where $\mu_{lm}^k \in \{0, \pm 1\}$, and where θ_{lm} are the coupled cluster amplitudes. Moreover, we denote $\hat{N}_{lm} = |\boldsymbol{\mu}_{lm}|$ as the number of non-zero elements in $\sum_k \mu_{lm}^k \sigma_n^k$.

Corollary 3 (Example: UCC). *Let H denote a molecular Hamiltonian of a system of M_e electrons. Consider the UCC ansatz as defined in Eq. (F1). If local Pauli noise of the form in Eq. (A5) with noise parameter q acts before and after every $U_{lm}(\theta_{lm})$ in Eq. (F1), then we have*

$$|\partial_{\theta_{lm}} \tilde{C}| \leq \sqrt{2} \hat{N}_{lm} N_H \|\boldsymbol{\omega}\|_\infty 2^{n/2} q^{L+1}, \quad (\text{F2})$$

for any coupled cluster amplitude θ_{lm} , and where $O = H$ in Eq. (A3).

Proof. Using the first-order Trotterization, the UCC ansatz can be represented as follows:

$$U(\boldsymbol{\theta}) = \prod_{lm} \prod_k e^{i\theta_{lm} \mu_{lm}^k \sigma_n^k}, \quad (\text{F3})$$

which is in the form of an ansatz that has correlated parameters. Then from Remark 1 it follows that

$$|\partial_{\theta_{lm}} \tilde{C}| \leq \sqrt{2} \hat{N}_{lm} N_H \|\boldsymbol{\omega}\|_\infty 2^{n/2} q^{L+1}, \quad (\text{F4})$$

where we used the fact that in Eq. (D5) $b = \hat{N}_{lm}$, $N_{st} = 1$, and $\|\boldsymbol{\eta}_{st}\|_\infty = 1$ for the UCC ansatz as in Eq. (F3). \square

G. Proof of Proposition 1

In this section we provide a proof of Proposition 1, which we now recall for convenience.

Proposition 1 (Measurement noise). *Consider expanding the observable O as a sum of Pauli strings, as in Eq. (4). Let w denote the minimum weight of these strings, where the weight is defined as the number of non-identity elements for a given string. In addition to the noise process considered in Fig. 5, suppose there is also measurement noise consisting of a tensor product of local bit-flip channels with $(1 - q_M)/2$ being the bit-flip probability. Then we have*

$$\left| \tilde{C} - \frac{1}{2^n} \text{Tr } O \right| \leq q_M^w G(n) \quad (\text{G1})$$

and

$$|\partial_{lm} \tilde{C}| \leq q_M^w F(n), \quad (\text{G2})$$

where $G(n)$ and $F(n)$ are defined in Lemma 1 and Theorem 1, respectively.

Proof. We prove in detail only the proposition about the gradient of the cost function. The proposition about the cost function is derived in an analogous manner.

As a model of measurement noise we consider a classical bit-flip channel applied to every qubit, such that the standard POVM elements get replaced by:

$$P_0 = |0\rangle\langle 0| \rightarrow \tilde{P}_0 = p_{00}|0\rangle\langle 0| + p_{01}|1\rangle\langle 1| \quad (\text{G3})$$

$$P_1 = |1\rangle\langle 1| \rightarrow \tilde{P}_1 = p_{10}|0\rangle\langle 0| + p_{11}|1\rangle\langle 1|, \quad (\text{G4})$$

where $p_{00} + p_{01} = 1$ and $p_{10} + p_{11} = 1$. Furthermore, we take this channel to be unital, such that $\tilde{P}_0 + \tilde{P}_1 = (p_{00} + p_{10})P_0 + (p_{01} + p_{11})P_1 = P_0 + P_1$ giving $p_{00} + p_{10} = 1$ and $p_{01} + p_{11} = 1$. Thus, there is only one free parameter q_M , and we set $p_{00} = p_{11} = \frac{1+q_M}{2}$, $p_{01} = p_{10} = \frac{1-q_M}{2}$. Note that without loss of generality we can assume $p_{00}, p_{11} > 1/2$, and hence $q_M \geq 0$. Overall:

$$P_0 = |0\rangle\langle 0| \rightarrow \tilde{P}_0 = \frac{1+q_M}{2}|0\rangle\langle 0| + \frac{1-q_M}{2}|1\rangle\langle 1| \quad (\text{G5})$$

$$P_1 = |1\rangle\langle 1| \rightarrow \tilde{P}_1 = \frac{1-q_M}{2}|0\rangle\langle 0| + \frac{1+q_M}{2}|1\rangle\langle 1|. \quad (\text{G6})$$

The equivalence between this classical channel and a quantum bit-flip channel is seen by writing $P_0 = \frac{\mathbb{1}+Z}{2}$ and $P_1 = \frac{\mathbb{1}-Z}{2}$, such that the bit-flip channel is equivalent to a shift in the Z operator: $\tilde{Z} = q_M Z$. This corresponds to the effect of a bit-flip channel $\mathcal{N}(\rho) = \frac{1+q_M}{2}\rho + \frac{1-q_M}{2}X\rho X$. Note that we have freedom here to choose the Pauli to be Y, or indeed any linear combination of X and Y.

The reasoning up to now applies only to measurements in the Z basis. However, in our model we do not consider a POVM, but the expectation value with respect to an Hermitian operator. This assumes the capability of performing measurements in any basis. If we assume that the classical bit-flip acts independently of the basis we choose to measure in, then we see that the corresponding quantum channel must be a depolarizing channel such that

$$\mathcal{N}(\sigma) = q_W \sigma, \quad (\text{G7})$$

This is a realistic assumption, as in actual quantum computer the basis of measurement would effectively still be the computational one, the only difference being an extra one-qubit rotation. Overall, we model measurement noise as a tensor product of such local depolarizing channels applied prior to measurement. The overall channel will be denoted by \mathcal{N}_M . From Eq. (G7) we have that

$$\mathcal{N}_M(O) = \sum_i \omega^i \mathcal{N}_M(\sigma_n^i) = \tilde{\omega} \cdot \sigma_n, \quad (\text{G8})$$

where $\tilde{\omega}$ is a vector of elements $\tilde{\omega}_i = q_M^{w(i)} \omega^i$, and where $w(i) = x(i) + y(i) + z(i)$ is the weight of the Pauli string. Here we recall that we have respectively defined $x(i)$, $y(i)$ and $z(i)$ as the number of Pauli operators X, Y, and Z in the i -th Pauli string. Let us now write the noisy cost function partial derivative as:

$$\partial_{lm} \tilde{C} = \text{Tr} [\mathcal{N}_M(O) \partial_{lm} \rho_L], \quad (\text{G9})$$

which can be represented in the Pauli basis as follows:

$$\partial_{lm} \tilde{C} = \frac{1}{2^n} \text{Tr} [(\tilde{\omega} \cdot \sigma_n)(\mathbf{g}^{(L)} \cdot \sigma_n)] \quad (\text{G10})$$

$$= \tilde{\omega} \cdot \mathbf{g}^{(L)}. \quad (\text{G11})$$

Then, we can write:

$$|\tilde{\omega} \cdot \mathbf{g}^{(L)}| \leq \sum_i |\tilde{\omega}_i| |g_i^{(L)}| \leq \sum_i q_M^{w(i)} |\omega_i| |g_i^{(L)}|. \quad (\text{G12})$$

Now defining w as the minimum weight, and N_O the number of the Pauli strings that compose the measurement operator O, we further loosen the bound:

$$|\tilde{\omega} \cdot \mathbf{g}^{(L)}| = |\partial_{lm} \tilde{C}| \leq q_M^w \sum_i |\omega_i| |g_i^{(L)}| \leq q_M^w N_O \|\omega\|_\infty \|\mathbf{g}^{(L)}\|_\infty. \quad (\text{G13})$$

Using $\|\mathbf{g}^{(L)}\|_\infty \leq \sqrt{2}N_{lm}\|\boldsymbol{\eta}_{lm}\|_\infty q^{L+1}2^{n/2}$, we get

$$|\partial_{lm}\tilde{C}| \leq \sqrt{2}q_M^w N_{lm} N_O \|\boldsymbol{\eta}_{lm}\|_\infty \|\boldsymbol{\omega}\|_\infty q^{L+1}2^{n/2} \quad (\text{G14})$$

$$= q_M^w F(n). \quad (\text{G15})$$

Now let us sketch how the proposition on the cost function is derived. Assuming $\text{Tr}[O] = 0$, can write

$$\left| \tilde{C} - \frac{1}{2^n} \text{Tr}[O] \right| = \mathbf{a} \cdot \tilde{\boldsymbol{\omega}}. \quad (\text{G16})$$

Therefore, in an analogous manner, we can write:

$$\left| \tilde{C} - \frac{1}{2^n} \text{Tr}[O] \right| \leq q_M^w N_O \|\boldsymbol{\omega}\|_\infty \cdot 2^{n/2} q^{L+1} \quad (\text{G17})$$

$$= q_M^w G(n). \quad (\text{G18})$$

Hence observables with $w \in \text{poly}(n)$ will suffer from an exponential decay in n of the cost function and its gradient. \square